DESIGN RECOMMENDATIONS FOR CONCRETE STRUCTURES PRESTRESSED WITH FRP TENDONS

FHWA CONTRACT

DTFH61-96-C-00019

Final Report

August 1, 2001

Prepared by

University of Wyoming

Charles W. Dolan

H.R. Hamilton III

Pennsylvania State University

Charles E. Bakis

And

University of Missouri - Rolla

Antonio Nanni

DESIGN RECOMMENDATIONS FOR CONCRETE STRUCTURES PRESTRESSED WITH FRP TENDONS

ABSTRACT

This report presents the state of development of fiber-based (non-metallic) reinforcement for prestressed concrete structures. It summarizes work in progress, work executed in this project and presents design recommendations for the use of FRP prestressing materials. The term fiber reinforced polymer (FRP) is used to identify this type of primary reinforcement used for prestressed concrete members. The material presented in this report includes a basic understanding of flexure and axial loaded prestressed members, bond of FRP tendons and a preliminary understanding of FRP shear reinforcement for prestressing applications. Specifications for testing FRP tendons are presented. Recommendations for AASHTO SPECIFICATIONS changes to incorporate FRP prestressing are presented in the results of this research.

PREFACE

This final report is prepared as a short course in the use of FRP prestressing for bridge structures. Each chapter is excerpted from research papers and student theses that were developed as part of this project. Volumes 2 and 3 of this report include the detailed reports and technical papers used to develop these design recommendations. Because the reports and papers are independent documents they are not formally part of the final report. They are available electronically as a CD included with the submission of the final report and on the University of Wyoming website. The web address is http://wwweng.uwyo.edu/civil/research/papers/. The table of contents for Volume 2 and 3 is included in the Final Report to assist the reader in locating sections of interest.

TABLE OF CONTENTS – FINAL REPORT

VOLUME 2 - TABLE OF CONTENTS

CHAPTER 2 – FLEXURAL STRENGTH OF FIBER REINFORCED POLYMER PRESTRESSED BEAMS…………………………………………………………113

VOLUME 3 – TABLE OF CONTENTS

J.   An Assessment of Flexural Behavior of CFRP Prestressed Beams Subjected to Incremental Static Loading

K.   Constructability and Performance of PC Members with FRP Tendon

L.   Investigation of Concrete Beams Post-Tensioned with Unbonded Carbon Fiber Reinforced Polymer Tendons

M.   **Applications of Fully Bonded FRP Tendons in Prestressed Concrete Structures**

1.0 INTRODUCTION

Fiber reinforced polymers (FRP) have been proposed for use in lieu of steel for reinforcement and prestressing tendons in concrete structures. The promise of FRP materials lies in their high-strength, lightweight, non-corrosive, non-conducting, and non-magnetic properties. In addition, FRP manufacturing offers a unique opportunity for the development of shapes and forms that would be difficult or impossible to fabricate with conventional steel materials. Lighter weight materials and preassembly of complex shapes can boost constructability and efficiency of construction. At present, the higher cost of FRP materials suggests that FRP use will be confined to applications where the unique characteristics of the material are most appropriate. Efficiencies in construction and reduction in fabrication costs will expand their potential market.

FRP reinforcement includes internal bars, grids and tendons. External reinforcement includes plates attached with adhesives. This report examines the internal prestressed reinforcement where the interaction of the FRP and the concrete is most acute.

One of the principle advantages of FRP reinforcement is the ability to configure the reinforcement to meet specific performance and design objectives. For example, FRP reinforcement may be configured in rods, bars, plates, and strands, Figure 1.1. Within these categories, the surface texture of the FRP reinforcement may be modified to increase or decrease the bond with the surrounding concrete. Unlike conventional steel reinforcement, there are no standardized shapes, surface configurations, fiber orientation, constituent materials and proportions for the final products. Similarly, there is no standardization of the methods of production, e.g., pultrusion, braiding, filament winding, or FRP preparation for a specific application.

Figure 1.1: Sample FRP Reinforcement Configurations

FRP reinforcement is typically made from one of three basic fibers. These fibers are aramid, carbon and glass. The selection of the fiber is primarily based on consideration of cost, strength, rigidity, and long-term stability. Within these fiber groups, there are numerous different performance characteristics available. For example, aramids may come in low, high and very high modulus configurations. Carbon fibers are also available with a large range of moduli; with upper limits four times that of steel. Of the several glass fiber types, glass-based FRP reinforcement is least expensive and generally uses either E-glass or S-glass fibers.

The resins used for fiber impregnation are usually thermosetting and may be polyesters, vinylesters, or epoxies. The formulation, grade, and physical-chemical characteristics of resins are practically limitless. The combinations of different fibers, resins, additives, and fillers make characterization of FRP reinforcement very difficult. Additionally, the fibers and the FRP composites are heterogeneous and anisotropic. Final tendon characteristics are dependent on fiber, resin and manufacturing process.

1.1 Organization and Limitations of This Report

This report is the result of a comprehensive research project that examined the use of fiber reinforced polymer prestressed tendons. This final Report is a summary of the research conducted in this project and ancillary related research. Appendix I contains detailed recommendations for testing, evaluating and classifying FRP tendons. Appendix II contains a first draft of recommended change to the AASHTO Design Specifications to incorporate the use of FRP tendons. Details of the research and the various source documents are given in Volume 2, prepared by the University of Wyoming and Volume 3 prepared by The Pennsylvania State University and the University of Missouri- Rolla. Volumes 2 and 3 are not formally part of the Final Report, however, references to the Volumes 2 and 3 are provided at the beginning of the sections of this report and the full Table of Contents of Volumes 2 and 3 are provided for the benefit of the reader.

The primary emphasis of this work is on pretensioned concrete applications. Information is provided for post-tensioned applications, as it is available. All work was conduced on simple span structures and no attempt was made to examine multiple span continuous structures. The authors feel that this work is relevant to simple span beams made continuous by placing reinforcement in the bridge deck and could be extrapolated to continuous beams. Secondary stresses in the deck, resulting from deck reinforcement continuity, will not affect the FRP performance. The report specifically makes no recommendations for moment resisting frame structures where ductility or large deformations are required for seismic loadings.

1.2 Historical Development of FRP Reinforcement

The concept of short glass fiber reinforcement in cements was first introduced in the 1930's but was not developed into long fiber reinforcement for nearly two decades. By the 1950's and 60's the U.S. Army Corps of Engineers was sufficiently interested in long glass fibers for reinforcement that a series of comprehensive reports was compiled under the direction of Bryant Mather [Mather 1955, Pepper 1959, Wines 1966]. Although these reports were generated, research and site applications were limited. In the 1970's corrosion of concrete structures, particularly bridge decks, led to a renewed interest in design strategies that would reduce structural susceptibility to corrosive environments. Interest continued to grow in the

1980's in the corrosion resistant properties of nonmetallic bars and tendons. The National Bureau of Standards (NBS)—now renamed the National Institute of Standards and Technology (NIST)—examined non-metallic rods for antenna guys. In the process they conducted some of the first research into anchorage of composite rods that became relevant to prestressed concrete application of FRP materials [NBS 1976].

With the exception of this project, the development of FRP reinforcement in the United States has been the result of individual investigator's efforts. Unlike Japan, there is no coordinated national research activity, and unlike the United Kingdom, Germany, and Holland, there have been no major corporations sponsoring coordinated or extensive development. Even with this lack of coordinated effort, considerable research and development has been accomplished. The National Science Foundation (NSF) has sponsored several independently submitted proposals from institutions such as such the University of Arizona, University of Michigan, Massachusetts Institute of Technology, Catholic University of America, Pennsylvania State University, University of California (Long Beach), West Virginia University, the University of Wyoming [FRP 1993], and Lawrence Technical University. These projects have led to an expanded understanding of FRP behavior. The U. S. Department of Transportation's Federal Highway Administration (FHWA) is also supporting research into FRP performance. Major projects at the University of California, Long Beach, University of California, San Diego and the University of West Virginia have examined FRP reinforcement and FRP composite construction. Researchers at the University of West Virginia have suggested guidelines for material selection and fabrication of fiberglass/polyester reinforcing rods. While not industry standards, these guidelines allow some unification of product quality. The Society of Plastics Industries and the American Society of Civil Engineers have established standards committees to address stand alone FRP products. In 1993, the FHWA initiated research into accelerated aging and standardized testing of FRP materials. Research Georgia Tech, Penn State and Catholic University of America examined accelerated aging evaluation of FRP reinforcement. Lawrence Technical University is currently developing a demonstration bridge using external unbonded FRP tendons.

In January 1991, the American Society of Civil Engineers sponsored a conference on Advanced Composites Materials in Civil Engineering Structures [Iyer and Sen 1991]. The conference examined many active research projects using FRP reinforcement. The Third Bridge

Engineering Conference, sponsored by the Transportation Research Board, included presentations of both FRP reinforcement and prestressing research [TRB 1991]. The Transportation Research Board formally established a committee to examine the use of FRP in bridge structures. This committee meets annually at the TRB Conference in Washington, DC, and serves as a valuable conduit for researchers, designers and interested parties to follow the development of FRP research in bridge structures. The American Concrete Institute (ACI) formed Committee 440, FRP Reinforcement, to investigate and promulgate knowledge regarding the use of FRP in concrete structures. In March 1993, ACI sponsored an International Symposium on FRP Reinforcement for Concrete Structures [Nanni and Dolan 1993]. Over 50 technical papers were presented or published. This conference led to the second International Conference on FRP Reinforcement for Concrete Structures in 1995 and the third conference in Sapporo, Japan, in October 1997 [Taerwe 1995, JSCE 1997]. In 1999 ACI Committee 440 sponsored the Fourth International Symposium in Baltimore [Dolan, Rizkalla and Nanni 1999]. Other societies including the Society for the Advancement of Material and Process Engineering (SAMPE) and the Society of the Plastic Industry (SPI) have been active in the area of FRP for construction use.

1.3 Canadian Activities

The Canadian Society for Civil Engineering Technical Sub-Committee on Advanced Composite Materials (ACM) was formed in 1989. One of this committee's first tasks was to organize a technical mission to Europe in 1991 to study research on and applications of FRP. The report on this mission (Mufti et al. 1991) presented a comprehensive state-of-the-art on advanced composite materials. In 1992, the committee sponsored a technical mission to Japan (Mufti et al. 1992). This activity also spawned a conference on Advanced Composite Materials in Bridges and Structures (ACMBS) held in Sherbrooke in 1992. The second conference in this series (ACMBS-II) was held in Montreal in 1996 and the third is scheduled for Ottawa in August 2000.

The ACMBS Network was formed in 1993 to enhance relationships between researchers and industry. This Network sponsored several technical missions, conferences, and workshops. The Intelligent for Sensing for Innovative Structures (ISIS Canada) Network was formed in 1995

to develop sensing technology for structures built with advanced composite materials. ISIS Canada has provided a strong focus for ACM research activity in Canada.

In addition to research, several demonstration projects have shown the potential of FRP applications. In 1993, a bridge was built in Calgary using FRP prestressing tendons incorporating fiber optic sensors (Rizkalla and Tadros 1994). This was the first bridge of its kind in Canada, and one of the first in the world. A second bridge incorporating both steel and FRP prestressing tendons was built in Headingley, Manitoba in 1997. Another demonstration project was the steel-free deck slab used in the Salmon River bridge in Nova Scotia in 1995. A similar steel-free deck slab was used in the rehabilitation of a bridge in Chatham, Ontario in 1996. FRP sheets have also been used to repair several structures including the Highway 10 overpass bridge in Quebec, the Champlain bridge in Montreal, the Webster parking garage in Sherbrooke, Quebec, and the Clearwater Creek bridge in Alberta.

Several researchers across Canada have been investigating applications of FRP prestressing tendons. Work at the University of Manitoba has emphasized carbon FRP tendons and has considered the behavior of prestressed beams under both service and ultimate conditions (Abdelrahman et al. 1995, Fam et al. 1997). Extensive studies on bond and transfer length have also been conducted. At the Royal Military College of Canada (RMC), work was done on aramid FRP tendons (McKay and Erki 1993), and more recently on carbon FRP tendons. Researchers at Queen's University have been investigating the low temperature and long-term behavior of beams prestressed with carbon FRP (Bryan and Green 1996). Additionally, the possibility of using carbon FRP rods to prestress bridge deck slabs was investigated (Braimah et al. 1996), and work on the transfer length of beams prestressed with carbon FRP was conducted (Soudki et al. 1997). Work at Queen's has focused on anchors for FRP tendons in collaboration with the University of Calgary. At the University of Sherbrooke, extensive investigations were conducted into the durability of FRP rods for reinforcing and prestressing concrete. The effects of temperature on beams prestressed with FRP tendons has been the focus of research at Concordia University, and applications of unbonded FRP tendons have been considered at the University of Windsor. Researchers at Carleton University and the University of Waterloo are also investigating applications of FRP prestressing tendons.

1.4 Japanese Activities

The Japanese have undertaken an extensive national program to examine the use of FRP reinforcement in concrete structures. This effort has lead to the development of several commercial tendon systems, many of which are discussed in the First international Symposium for FRP Reinforcement in Reinforced Concrete Structures (Nanni and Dolan 1993) and in the Japanese Society of Civil Engineers (JSCE) journals (JSCE 1996).

Around 1980, research and development began in Japan on production techniques for FRP reinforcement and its application to concrete structures. This R&D originally focused on the development of FRP reinforced concrete members that used FRPs instead of reinforcing steel and prestressing steel.

In building (architectural) engineering, the Research Committee on Continuous Fiber Composite Materials was organized into the Architectural Institute of Japan in 1988. Three years later, they had formulated items and methods for evaluating FRP concrete. Based on these results, the Ministry of Construction conducted over 30 experimental studies on these materials at the Building Research Institute and elsewhere in its Comprehensive Technological Development Project titled "Technological Development of New Construction Materials." In 1993, the first design guidelines in the world were established for FRP reinforced and prestressed concrete buildings. The Japanese version of the guideline was released in 1995, while the English version (Sonobe 1997) was published in 1997.

In civil engineering, the Research Committee on Continuous Fiber Reinforcing Materials was organized into the Japan Society of Civil Engineers in 1989, conducting surveys and research on methods for evaluation and application. The committee was reestablished in 1992 to formulate guidelines for design and construction. The Japanese version was completed in 1996, while the English version (JSCE 1996) came out in 1997. In the above-mentioned Comprehensive Technological Development Project, the Public Works Research Institute and other organizations developed techniques for using these new materials in cables for bridges. The research ended in 1993 and the results were made public in Japan and in limited English language proceedings.

The decline in the Japanese economy in the 1990's has slowed the Japanese development program and has curtailed the availability of many Japanese products for evaluation and testing in the US. Current developments in Japan are addressed by Fukuyama (1999).

1.5 European Activities

In the 70's, research activities started in Germany on glass FRP-based prestressing tendons because GFRP appeared less appropriate for reinforced concrete due to its low modulus of elasticity. In 1978, a joint venture between German contractor Strabag-Bau and German chemical producer Bayer resulted in the GFRP bars and an anchorage for post-tensioning applications. These tendons were incorporated in several bridges in Germany and Austria. However, after various transition stages, Strabag stopped its activities in this field in the early '90s. In The Netherlands in 1983, AKZO, a chemical producer, and HBG, a contractor, jointly developed aramid fiber (AFRP) based prestressing elements.

Of the projects financially supported by the European community, the BRITE/EURAM project, titled "Fiber Composite Elements and Techniques as Non-Metallic Reinforcement for Concrete," started November 1991 and ended in 1996. The Universities of Braunschweig and Ghent and industrial partners from Germany and The Netherlands investigated performance characteristics and structural aspects of FRP for prestressed and reinforced concrete members.

The EUROCRETE project, a pan-European collaborative research program with partners from the United Kingdom, The Netherlands, Switzerland, France, and Norway, began in December 1993 and ended in 1997. This project included material development, research on durability in aggressive environments, determination of structural behavior, and development of design guidance, techno-economic and feasibility studies. The project included construction of demonstration structures.

In December 1997, a four-year training and mobility of researchers network project, titled "Development of Guidelines for the Design of Concrete Structures, Reinforced, Prestressed or Strengthened with Advanced Composites," started (1 TMR). This so-called "ConFibreCrete Network" is comprised of 11 teams from nine different European countries. The network also supports the work of *fib* (International Federation for Structural Concrete) Task Group 9.3 in developing design recommendations (*Fib*).

At the European level, unified design guidelines for FRP reinforcement are under development. A task group with this aim was established at the end of 1996, within the former CEM (Euro-International Concrete Committee). Since the merger of CEB and FIP (International Federation for Prestressed Concrete), this task group is integrated in the new fib (International Federation for Structural Concrete). Within Task Group 9.3 of fib Commission 9, design guidelines are elaborated for concrete structures reinforced, prestressed, or strengthened with FRP, based on the design format of the CEB-FIP Model Code and Eurocode 2. Recent activities in Europe were summarized by ACI in October 1999 (Taerwe 1999).

1.6 References

Abdelrahman, A.A., Tadros, G., and Rizkalla, S.H., (1995). Test Model for the First Canadian Smart Highway Bridge. ACI Structural Journal, Vol. 92, No. 4, July-Aug., pp. 451-458.

Braimah, A., Green, M.F., and Soudki, K.A., (1996). Eliminating Steel from Bridge Deck Slabs by Combining CFRP Tendons with Polypropylene FRC. Proceedings of the Advanced Composite Materials in Bridges and Structures (ACMBS) Conference, Montreal, Quebec, 11-14 Aug., pp. 735-742.

Bryan, P.E., and Green, M.F., (1996). Low Temperature Behaviour of CFRP Prestressed Concrete Beams. Canadian Journal of Civil Engineering, Vol. 23, No. 2, April, pp. 464-470.

Dolan, C.W., Rizkalla, S., and Nanni, A., editors, (1999). Fourth International Symposium On Frp Reinforcement For Concrete Structures SP 188, American Concrete Institute, Farmington Hills, MI.

El-Badry, M., editor (1996). Proceedings of the Second International Conference on Advanced Composite Materials in Bridges and Structures (ACMBS-II). Sherbrooke, Canada, Oct., Canadian Society for Civil Engineering.

Fam, A.Z., Rizkalla, S.H., and Tadros, G., (1997). Behavior of CFRP for Prestressing and Shear Reinforcements of Concrete Highway Bridges. ACI Structural Journal, Vol. 94, No. 1, Jan.-Feb., pp. 77-86.

Fib (International Federation for Structural Concrete) Task Group 9.3, "FRP Reinforcement for Concrete Structures." http://allserv.rug.ac.be/~smatthys/fibTG9.3

FRP Research (1993). FRP INTERNATIONAL, S. Rizkalla, Ed., Winnipeg, Canada, Vol. 1, No. 1, January, p. 5.

Fukuyama, H., (1999) :FRP Composites in Japan," Concrete International, American Concrete Institute, Farmington Hills, MI, vol 21, n0. 10, October. pg. 29.

Iyer, S. L. and Sen, R., eds. (1991). Advanced Composites Materials In Civil Engineering Structures. American Society of Civil Engineers, NY, NY, Specialty Conference, Jan 31 - Feb 1

JSCE, (1996). Research Committee on Continuous Fiber Reinforcing Materials: Recommendation for Design and Construction of Concrete Structures Using Continuous Fiber Reinforcing Materials, Concrete Library No. 88, Japan Society of Civil Engineers, Tokyo, Japan, September.

Mather, B. and Tye, R. V. (1955). "Plastic-Glass Fiber Reinforcement for Reinforced and Prestressed Concrete; Summary of Information available as of July 1 1955". Technical Memorandum No. 6-421, Report 1, Corps of Engineers, Waterways Experiment Station, Vicksburg, MS.

McKay, K.S., and Erki, M.A., (1993). Flexural Behavior of Concrete Beams Pretensioned with Aramid Fibre Reinforced Plastic Tendons. Canadian Journal of Civil Engineering, Vol. 20.

Mufti, A.A., Erki, M.A., and Jaeger, L.G., editors, (1991). Advanced Composite Materials with Application to Bridges. Canadian Society for Civil Engineering, Montreal, Canada.

Mufti, A.A., Erki, M.A., and Jaeger, L.G., editors, (1992). Advanced Composite Materials in Bridges and Structures in Japan. Canadian Society for Civil Engineering, Montreal, Canada.

Nanni, A and Dolan, C.W., eds. (1993). International Symposium On Frp Reinforcement For Concrete Structures. American Concrete Institute, Detroit, MI

NBS (1976). "Non-Metallic Antenna Support Materials Pultruded Rods for Antenna Guys, Catenaries and Communications Structures". Technical Report AFML-TR-76-42, National Bureau of Standards, Washington, DC pp. 126.

Neale, K.W., and Labosierre, P. editors, (1992). Proceedings of the First International Conference on Advanced Composite Materials in Bridges and Structures (ACMBS-I). Sherbrooke, Canada, Oct., Canadian Society for Civil Engineering.

Pepper, L., and Mather, B. (1959). "Plastic-Glass Fiber Reinforcement for Reinforced Prestressed Concrete; Summary of Information from 1 July 1955 to 1 January 1959". Technical Memorandum No. 6-421 Report 2, Corps of Engineers, Waterways Experiment Station, Vicksburg, MS.

Rizkalla, S.H., and Tadros, G., (1994). A Smart Highway Bridge in Canada. Concrete International, June.

Sonobe, Y. et al, (1997): Design Guidelines of FRP Reinforced Concrete Building Structures, Journal of Composite for Construction, American Society of Civil Engineers, pp. 90-115, Reston, U.S., August.

Soudki, K.A., Green, M.F., and Clapp, F.D., (1997). Transfer Length of Carbon Fibre Rods in Precast Pretensioned Concrete Beams. PCI Journal, Vol. 42, No. 5, pp. 78-87.

Taerwe, L. and Matthys, S. (1999). "FRP for Concrete Construction: Activities in Europe," Concrete International, American Concrete Institute, Farmington Hills, MI, vol 21, no. 10, October. pg. 33.

1 TMR (Training and Mobility of Researchers) Network, "Development of Guidelines for the Design of Concrete Structures, Reinforced, Prestressed or Strengthened with Advanced Composites (ConFibreCrete)." http://www.shef.ac.uk/~tmrnet

TRB (1991). Third Bridge Engineering Conference. Transportation Research Record, No. 1290, volumes 1 and 2, Transportation Research Board, Washington, DC

Wines, J. C., Dietz, R. J., and Hawley, J.L. (1966). "Laboratory Investigation of Plastic-Glass Fiber Reinforcement for Reinforced and Prestressed Concrete," Report 2. Corps of Engineers, Waterways Experiment Station, Vicksburg, MS.

Wines, J.C. and Hoff, G. C. (1966). "Laboratory Investigation of Plastic-Glass Fiber Reinforcement for Reinforced and Prestressed Concrete", Report 1. Corps of Engineers, Waterways Experiment Station, Vicksburg, MS.

2.0 FRP TENDONS AND ANCHOR SYSTEMS

Material for this section is excerpted from Volume 3, Section A

This section presents commercially available tendons and anchorage systems as of 1997. The decline of the Japanese economy and the lack of any sustainable series of FRP prestressing have resulted in no new tendon or anchor development in the US. Properties and characteristics of available tendon/anchor systems are summarized in Table 2.1 and are based on the manufacturer's published data. The trade names of the products are used for clarity and historical perspective. The list order is based on type of anchor system (i.e., wedge, molded, and spike anchors). Within each type of anchor system, the list has been arranged alphabetically by, first, fiber type (i.e., aramid, carbon, glass) and, second, by product name. Table 2.1 has been developed from historical data. Not all tendons are currently available and the properties of the tendons are subject to change.

Table 2.1: Manufacturer's material properties

Tendon	Type	Nominal Diameter (mm)	Cross Section (mm^2)	Young's Modulus (GPa)	Ultimate Load (kN)	Ultimate Strain (percent)	Density (g/cm^3)	Poisson's Ratio
Arapree	f200 000	7.5	44.2	62.5	66.6	2.40	1.25	0.38
Arapree	f400 000	10.0	78.5	62.5	115.5	2.40	1.25	0.38
FiBRA	FA13	12.7	127.0	68.6	176.4	2.00	1.62	0.60
Carbon Stress	Flat strip	17.5 x 1.65	28.9	150.0	54.0	1.60	N/A.	N/A
Carbon Stress	Round	5.4	22.9	160.0	49.0	1.60	N/A	N/A
Leadline	Indented	7.9	46.1	150.0	104.0	1.30	1.67	N/A
Technora	Spiral Wound	8.0	50.2	54.0	86.2	3.70	1.30	0.35
CFCC	1x7 12.5	12.5	76.0	137.3	142.0	1.57	3.31	N/A
Lightline	Strand	10.5	67.6	51.8	90.8	2.50	N/A	N/A
Parafil	Type G	13.5	86.6	120.0	105.0	1.50	1.44	N/App.

(Source: Nanni et al. 1996 and 1996a)

(Note: 1.0 in = 25.4 mm; 1.0 MSi = 0.145 GPa; 1.0 lb/cu. ft = 0.016 g/cm^3)

2.1 Description of Commercial Tendons and Anchors

Arapree. Arapree was a combined development of AKZO Chemicals and Hollandsche Beton Groep (HBG), the Netherlands. The manufacturing rights have been transferred to Sireg S.p.A., an Italian industry. Arapree consists of aramid (Twaron) fibers embedded in epoxy resin. Two cross-section types are available in the marketplace: rectangular and circular. The former may be easier to grip with a wedge anchor system (Gerritse and Werner 1988).

The anchoring system developed for Arapree, both flat and round rod types, consists of a tapered metal sleeve into which the tendon is either grouted (post-tensioning application) or clamped between two wedges. The wedge anchor, designed primarily for temporary use, is comprised of a steel socket and two semi-cylindrical tapered wedges made of Polyamide PA6. The outer surface of the wedges and the inner surface of the metal socket are smooth and non-coated. The inner surface of the wedge trough, which holds the tendon is similarly smooth and gripping of the tendon, relies solely on the frictional resistance provided by the plastic.

FiBRA. Mitsui Construction Company of Japan produces an FRP rod known as FiBRA. Braiding fiber tows followed by epoxy resin impregnation and curing form the rod. Different types of fibers can be used, with aramid being the most common. Depending on small variations in the manufacturing process, two types of rod, rigid and flexible, are produced. Rigid rods are mainly used for concrete reinforcement, whereas flexible rods, which can be coiled, are used as prestressing tendons (Tamura 1993).

FiBRA has two different types of anchoring system: a resin-potted anchor used for single tendon anchoring, and a wedge anchor for either single or multiple tendon anchoring. The latter was evaluated in this project. This anchor is made of four steel wedges (held together by an O-ring) that slip inside a steel cylinder with a conical interior surface. Grit is applied to the inner surface of the wedges. The exterior surface of the wedges and the interior surface of the steel cylinder are coated with a dry lubricant to assist in seating and removal of the anchor.

Carbon Stress. Carbon Stress is the trade name of a prestressing tendon manufactured by Nederlandse Draad Industrie, a subsidiary of the Dutch steel producer Hoogovens. The original technology for this prestressing system was developed by AKZO Chemicals and is similar in manufacturing to Arapree. Both bar types are formed through pultrusion of epoxy-impregnated

carbon fibers. The flat bar is dimpled with a hatched pattern to create a better bonding surface. The round bar is coated with sand. Both types of tendons were obtained for testing.

Carbon Stress employs anchoring devices similar to those of Arapree. A difference is in a dry lubricant coating on the exterior surface of the plastic wedges to assist in setting of the wedges. This also aids in removal of the wedges after use. In addition, the manufacturer prepares wedges for flat tendons with a sand-coated surface in the grip zone. The wedges for the round tendons come with instructions to apply a layer of epoxy and sand into the groove that holds the tendon. In both cases, the function of the sand coating is to increase the gripping capability of the anchor.

Leadline. Mitsubishi Kasei Corporation of Japan has developed a carbon FRP rod called Leadline that is pultruded and epoxy-impregnated. There are several varieties of Leadline rods that differ in pattern and method of fabrication of their surface deformations. Smooth rods have no surface deformations. Indented rods have two shallow helical depressions in the surface which spiral in opposite directions. Ribbed rods have either raised helical windings similar to the indented pattern or a circumferential winding transverse to the longitudinal axis of the rod.

Leadline utilizes a modified wedge system to anchor the tendons. The modification comes in the form of an aluminum sleeve that fits between the wedges and the tendon. The sleeve has four independent arms that extend along the length of the tendon. The wedges are placed around the sleeve such that the gap between adjacent wedges falls over the solid portion of the sleeve. The sleeve is intended to spread the stresses imposed on the tendon by the wedges. A plastic film is placed around the whole assembly to secure the multiple pieces together for insertion into the steel socket.

Technora. Technora rod is a product jointly developed by Sumitomo Construction Company and Teijin Corporation, both of Japan. Named for the brand of aramid fiber used in its manufacture, Technora is a spirally-wound pultruded rod impregnated with a vinyl ester resin (Noritake et al. 1993). Manufacturing of a spirally-wound tendon begins with pultrusion the impregnated straight bundles through an unheated die. Identical fiber bundles are wound spirally around the rod to produce a deformed surface. Longitudinal fiber bundles are added to the outer surface before a second spiral winding is added. The product is then cured in an oven.

Technora tendons employ either wedge type or potted type anchorages. Anchorages for a single rod or multiple rods numbering from 3 to 19 rods are available. A screw thread is cut into the outer surface of the housing so that the anchor can be secured with a nut onto a bearing plate. An 8-mm (0.31-in) diameter, spirally-wound rod with potted-type anchors installed by the manufacturer was used in this project.

CFCC. Carbon Fiber Composite Cable (CFCC) was developed by Tokyo Rope and Toho Rayon Co., both of Japan. The cable is formed by twisting a number of small-diameter rods (e.g., 7, 13) similarly to a conventional stranded steel tendon (Santoh 1993). Materials used for CFCC include PAN-based carbon fiber and epoxy resin developed by Tokyo Rope. Multiple pieces of prepreg (i.e., semi-hardened tows with a resin precursor) are made into a bundle that is treated with a proprietary coating and formed into a small-diameter rod. A number of these rods are then stranded and formed into a composite cable that is heated and cured to form the finished product. The coating protects individual rods from UV radiation and mechanical damage while increasing bond characteristics with concrete.

The manufacturer classifies CFCC anchoring methods as resin filling and die cast methods. The anchoring systems are chosen based on the intended application. The resin-filling method bonds the cable to a steel cylinder utilizing a high-performance epoxy. These cylinders can be threaded as necessary to allow anchoring with nuts. The die cast method attaches the cable to a steel tube by means of a molten and die-molded alloy. Steel wedges clamp the steel tube similarly to steel tendon systems.

Lightline. Lightline cable is available from Neptco, Inc. This FRP tendon is stranded from seven individual rods (one central rod surrounded by six others), mimicking a conventional 7-wire steel strand. The individual rods were simply twisted together and held in place by plastic straps or a resin binder. The Lightline cable is a composite of E-glass fiber and epoxy resin with properties as given in Table 2.1.

The manufacturer had not developed the anchoring system to be utilized with this particular tendon. A resin potted anchor is threaded on the outside to receive a matching nut could be used to complete the tendon.

Parafil. Linear Composites of England is the producer of a parallel-lay rope composed of dry fibers contained within a protective polymeric sheath (Burgoyne 1988). Parafil was

originally developed in the early 1960's to moor navigation platforms in the North Atlantic. The cross-sectional area of the rope used in this project is based on a 10.5-mm (0.41-in) diameter, determined by subtracting the sheath thickness from the nominal diameter. Parafil has several features that distinguish it from other prestressing systems: it cannot be bonded to concrete; it contains no resin; and it was not initially developed for prestressing. Nevertheless, it has been used for prestressing concrete on a number of occasions.

Parafil ropes are anchored by means of a barrel and spike fitting, which grips the fibers between a central tapered spike and an external matching barrel. It has been suggested that aluminum alloy, galvanized mild steel, stainless steel and other materials may be used for the anchors since this scheme takes advantage of the fibers of the rope simply being tightly packed in the protective outer sheathing. Research is in progress to develop an all composite anchor.

2.2 Discussion of Anchor Performance

Anchor types can be divided into three groups: wedge, resin/grout potted, and spike systems. The wedge systems can be further subdivided into: direct contact (plastic and steel wedges) and systems utilizing a sleeve. The potted anchors group varies depending on the internal configuration of the socket: straight, linearly tapered, and parabolically tapered sockets. Only one spike anchor was considered. The following observations are made for the three anchor groups:

- Wedge Anchors. Grit should be present on the wedge surfaces to ensure proper gripping of the tendons. This observation is drawn from comparisons between the Carbon Stress and Arapree tendons, both of which utilize plastic wedges. The Carbon Stress system with applied grit did not show the slippage exhibited by the untreated Arapree wedges. Steel wedges induce some local damage to the tendon even though there was no indication of loss of efficiency. Systems with a dry-lubricated outer wedge surface are easier to take apart than other systems, though both required use of force to free the wedges.

- Resin/Grout Potted Anchors. Potted anchors often fail through pullout of the tendon from the resin/grout anchor without rupture of the tendon. The parabolic system showed splitting and cracking of the resin plugs. The potted anchors are the easiest to

setup for testing when they are pre-installed. The practical drawbacks include precutting the tendons to length and the curing time for the resin/grout.

● Spike Anchors. The spike anchors used with the dry fiber ropes work relatively well. This system requires field setup time, which resulted from the combination of removal of the plastic sheath, combing and spreading of the individual fibers and proper placement of the spike with a uniform distribution of fibers all around it.

2.3 References

Burgoyne, C.J., (1988) "Structural Applications of Parafil Rope, "Symposium on Engineering Applications of Parafil Rope," C. J. Burgoyne, Ed., Imperial College, London, 6 January, pg. 39-47.

Nanni, A., C.E. Bakis, E. O'Neil, and T.O. Dixon, (1996) "Short - Term Sustained Loading of FRP Tendon-Anchor Systems," Construction & Building Materials, Vol. 10, No. 4, pp. 255-266.

Nanni, A., C.E. Bakis, E. O'Neil, and T.O. Dixon, (1996) "Performance of FRP Tendon-Anchor Systems for Prestressed Concrete Structures," PCI Journal, Vol. 41, No. 1, Jan.-Feb., pp. 34-44.

Gerritse and Werner (1988) ARAPREE The prestressing element composed of resin bonded Twaron fibers, Holland Betron Groep nv, The Netherlands.

Tamura, T., Kanda, M. and Tsuji, Y. (1993) "Applications of FRP Materials to Prestressed Concrete Bridges and Other Structures in Japan" PCI Journal, Ed., George D. Nasser, July-August, pp. 50-58.

Noritake, K., Kakihara, R., Kumagai, S., Mizutani, J., (1993). "Technora, an Aramid FRP Rod" FRP Reinforcement for Concrete Structure: Properties and Applications, A. Nanni, ed., Elsevier Science Publishers B.V., Amsterdam.

Santoh, N., Kimura, H., Enomoto, T., Kiuchi, T., Kuzuba, Y., (1993). "Report on the Use of CFCC in Prestressed Concrete Bridges in Japan" Fiber-Reinforced-Plastic Reinforcement for Concrete Structures, A. Nanni, C. Dolan, ed., American Concrete Institute, United States.

3.0 TENDON DEFINITION

Material for this chapter is excerpted from Volume 2 Chapter 1.

A uniform method of defining the tendon strength is needed for design purposes. This section defines the "strawman" tendon used in the study, the methods of testing the tendon to establish tensile design strength and presents a detailed specification for use in defining tendon capacity.

3.1 Development of Tension Testing Procedure

A testing procedure is required to establish the various tensile strength capacities and material properties of FRP tendons. The procedure must identify the key parameters associated with the design of prestressed structures using a simple process that is reliable, repeatable and easily completed. The output must be the stress, strain, and modulus of elasticity of the tendon and the statistical variability of the tendon.

FRP tendons have stress-strain distributions that are nearly linear to failure. Consequently, this there is no redistribution of stresses due to yield of the material as occurs in steel. Steel tendons are typically stressed to 85 percent of their yield stress or about 0.005 strain. Allowable stresses in FRP tendons tend to be lower due to stress-rupture limitations as stresses fall into the prestress range of 40-60 percent of their ultimate strength and is discussed later in this report. This lower range of allowable stress might be misleading as actually it represents a corresponding strain between 0.008 and 0.012, or 1.5 to 2.5 times the prestressing strain of steel. The total strain at failure can range between 0.016 and 0.060 depending on the fibers used in the tendons.

This chapter develops testing specifications by identifying key parameters to be defined and/or tested. A draft testing specification is provided in Appendix I that summarizes the recommended testing methods. The draft specification has been submitted to ASTM committee D30.02.02 for consideration and development as an ASTM Standard.

Classification of Tendon

The first step in developing testing procedures is to clearly define the material that is being tested. Because of the wide variety of fibers, resins, shapes, and sizes used in FRP tendons it is imperative that a common classification system be developed. The format of the specification should contain enough information that the tendon is succinctly quantified. The draft FIP report suggests that there may be too many variables to successfully achieve this (FIP 92). For example, the exact fiber type of carbon can specifically be referred to as high, medium, or low strain carbon. Virtually all parameters have some detailed anomaly that could be specified. Alternatively, having a common performance requirement eliminates most of these variables as only the performance results would be recorded.

The Japanese have developed a system to define the FRP tendon used. The system identifies the type of fiber used and labels it as shown in Table 3.1.

Table 3.1 - Fiber Identification

Fiber Type	Identification
Glass fiber	G
Aramid Fiber	A
Carbon Fiber	C
Vinylon Fiber	V
Multiple Fibers	*

Where the * indicates that in a tendon using multiple fibers, the first letter of the two fibers making up the material will be used with the dominant fiber going first (e.g. CG for carbon/glass composite with carbon having the larger volume). Next, the Japanese identify the configuration of the tendon by the type of surface and/or shape that is used. Figure 3.1 shows the variety of configurations.

Category	Rod	Strand	Braided	Lattice	Rectangle
Symbol	R, D*	S	B	L	R
Configuration					

Figure 3.1 - Tendon Surface Configurations

In Figure 3.1 the * in the rod section indicates that there can be rods with a smooth surface (denoted R) or with deformed surfaces (D). The system finally classifies the rods in terms of the nominal diameters and volume fractions.

While this system can be used as a general method to classify tendon types, it does not provide specific information that is useful for design. A format can be developed that is similar to the Japanese, but also includes the strength of the material and the relative bond performance as well. The combination of the fiber type and the tendon structure will allow determination of the ultimate strength or strain capacity.

The bond performance will be assigned a value relative to a common testing material. Within this project the baseline tendon is the Strawman tendon described below. A preliminary example of a tendon description could be as follows: GS-12/1 for a stranded glass tendon with a 12 kN ultimate load and type 1 bond capacity. The Strawman would be CD-22/1, that is a carbon strand with a solid circular cross section, deformed surface, 22 kN design capacity and type 1 bond.

Length

Specifying the length required for a test specimen is an important parameter to developing consistently reproducible and reliable data. Tests by Castro et al. have shown that there is no significant statistical influence of varying the length of the tensile specimen between 40 and 70 diameters (Castro 97). Japanese recommendations specify that the length of the test piece shall be defined as the length of the test section added to the length of the anchoring section. The test section must be greater than 100 mm (4 in) and greater than 40 bar diameters. The recommendations are based on tests conducted by various organizations and a complete discussion on the subject is available in the commentary portion of the recommendations (JSCE 97).

Discussions of testing procedures for FRP tendons recommend that the specimen length should normally be substantially longer than the minimum requirement in order to minimize bending stresses due to minor grip eccentricities. However, this minimum requirement is not specified. Guidance is only given for the gauge length over which strain measurements occur. Therefore, in testing for this research the specimen length was defined as the distance between anchorages and must be a minimum of 40 bar diameters or 100 mm (4 in).

Tendon Dimensions

Calculation of the strength capacity and the modulus of elasticity require determination of the testing sample dimensions. ASTM D3916 specifies that the diameter of a bar be measured

with a micrometer at "several points along its length," noting the average and minimum values. While this appears to be a simple task, often times it is impractical because of the presence of surface deformations on the bars. Castro reported on a better approach where the diameter is determined from the mass, length, and density of a portion of the bar. The research examined the minimum length required to obtain a representative density by placing a sample in a pycnometer filled with water and measuring the displacement. It was concluded that a sample 200 mm (8 in) long gave accurate results (Castro 97).

The testing procedures must be developed so that testing can be carried out in a simple fashion. Thus using the pycnometer method would only be required in an extreme case where the surface of the sample was severely ribbed or deformed in such a way that it is impractical to obtain accurate micrometer readings. The process will be simplified by requiring tendon measurement to be recorded using a micrometer reading to at least 0.025 ±0.000 mm (0.001±0.000 in.), at three points along the test length with the average value recorded. Manufacturers have recorded the values for the dimensions and typically report a nominal diameter. For testing purposes validation of the exact dimensions shall be taken to produce accurate results. Providing load versus strain results eliminates the need for specific cross-sectional dimensions.

Anchorage

In addition to the anchors described in chapter 2, an expansive cement anchor was tested. The expansive cement anchor consists of an FRP tendon centered in a steel pipe. Highly expansive cement, as is used in concrete demolition, is poured into the pipe. The expansion of the cement compression bonds the tendon in the pipe. Only the expansive cement anchorage system proved useful for all testing procedures and is recommended for incorporation in an ASTM Standard. The expansive cement anchor is also adaptable to all universal test machines. Manufacturers may use proprietary anchors, however, the test results and applications must specify and use the same anchor.

Conditioning

Conditioning of specimens, as described by ASTM D618, is undertaken in order to bring a material into equilibrium with normal or average room conditions, to obtain reproducible results, or to subject the sample to abnormal conditions. For development of testing procedures

that result in obtaining reproducible results, a common procedure would be to include conditioning. FIP reports that FRP materials will have the highest strength immediately after production when moisture content is at a minimum. Exposure to moisture leads to small, reversible reduction of strength. The FIP studies have concluded that storage of the tendons for 1 to 2 weeks at a temperature of 20 C (68 F) and a relative humidity of 65% will standardize the moisture content in the polymer (FIP 92). The Canadian code states for tendon conditioning the requirements would be a minimum of seven days at a temperature not exceeding 20 C and relative humidity not less than 50%. The Canadian code is consistent with ASTM D5229 for testing of composite materials.

The Japanese, however, do not mention any need for a conditioning procedure. The only mention of tendon preparation is a statement that any method that will cause changes in the material properties (such as deformation, heating, or outdoor exposure to ultraviolet rays) must be avoided. This indicates that any conditioning procedure would be adequate as long as the properties are not compromised.

3.2 Testing Setup

Equipment

To expedite the use of FRP products in prestress applications a testing procedure must be developed that will be general so that a wide variety of testing equipment will be suitable for testing FRP tendons. To achieve a standard that is widely accessible, the equipment used in this project was a classical Tinius-Olsen Universal test machine with confirmation testing on an Instron 1334 Universal test machine. The equipment meets the required ASTM specifications. ASTM E4 provides the requirements for a load verification procedure.

Strain Indicating Devices

Strain data is needed for determination of the strain capacity and the modulus of elasticity of the tendon. Either a strain transducer or an extensometer may record the strain. With FRP tendons it is imperative that the attachment of these devices does not cause damage to the specimen surface because small defects in the surface can impair the strength of the specimen. The orientation of the devices will depend on the property that is to be determined. For the modulus of elasticity of the material the device must be oriented so that the longitudinal strain is

measured only. Determination of Poisson's ratio requires the specimen to be instrumented to measure strain in both longitudinal and transverse directions. The following sections discuss two types of strain indicating devices.

Strain transducers refer to electrical strain gages. Problems can arise in using electrical strain gages on FRP materials. Surface preparation in accordance with ASTM standards can cause damage to the reinforcing fibers due to preparation of the matrix materials. The damage in turn may result in improper specimen failures. Tendon surface and alignment, for example braided tendons, preclude many strain gage applications. Experimental application of strain gages on the strawman tendon was not satisfactory due to the deformed surface.

Extensometers provide a superior method to measure the strain on a FRP tendon than do strain gages. Extensometers for this procedure are limited to a strain gage based apparatus, linear variable differential transformer (LVDT), and a linear resistance potentiometer (linear pot). The extensometer is attached directly to the surface in a manner that does not damage the tendon. The use of three longitudinal extensometers uniformly spaced around the circumference of the tendon enables the assessment of bending about any axis and is recommended for a standard test method. Special diametral-type extensometers are able to measure transverse strain. Because tendons are typically 12.7 mm (0.5 in) in diameter the range over which the strain is recorded is small and accuracy suffers.

The explosive failure of an FRP tendon can damage extensometers. This research used linear potentiometers. The slight loss in precision was more than satisfactory when the cost of replacement instrumentation is considered.

Testing Conditions

Defining testing conditions encompasses a wide variation of allowable ranges. The FIP report states that during prestressing operations tendons endure temperature changes between –30C to 80C (-22 to 176F). Within this range the tensile strength of the tendon is not adversely affected (FIP 92). For abnormal conditions, the test will be dependent on the type of environment the tendon will be placed. Japanese testing guidelines limit the range of temperature from 5C to 35C (41 to 95F).

Loading Rate

The loading rate used for the tension test can affect the test values due to rate sensitivity of materials and temperature-time effects particularly in glass and aramid fiber composites (Mandell and Meier 1983; Roylance and Roylance 1981). It is necessary to establish suitable limits for the speed of a test when dealing with materials in which the differences resulting from the use of various speeds are of such magnitude that the test results are unsatisfactory for determining the acceptability of the material. Defining suitable limitations for speed of testing are done in various manners that are dependent upon the material and the use for which the test results are intended. Experimental data gathered in this program shows the minimal variations in the results due to loading rates if the time between initial loading and failure between 3 and 5 minutes.

Modes of Failure

When approaching failure, individual fibers break due to variability in individual fiber surface defects. This leads to interfacial slip between the broken fiber and the matrix, and consequently stress magnification in the adjacent fibers. Since the interfacial bond is still effective, tensile stress in the broken fiber along the bond transfer length will gradually build-up. If the bond strength is exceeded, delamination of the fiber from the matrix will commence and propagate. With interfacial bond lost progressive fiber fracture will occur leading to overall failure (FIP 92).

Because of the nature of the FRP materials, there can be a variety of unwanted failures within a test specimen. Anchorage can cause premature failure in the tendons and defining adequate anchors is critical. Poor alignment of the tendon in the grips or the anchorage causes bending at the anchor that may cause premature failure, as well as inaccurate modulus of elasticity determination. These failures can be controlled and the testing procedures define procedures to attempt to ensure proper failure of the specimen, and therefore accurate tensile data. Reports on the testing must include the mode of failure of the specimens.

Reporting Results

The final report must include all relevant test information. Appendix I contains the information listed in the testing procedures developed and a sample report on the Strawman tendon.

3.3 Statistical Evaluation

Experimental procedures for measurements of various quantities will always exhibit some variation if the measurements or tests are repeated. This variability can be attributed to two causes. First, the specimens being examined can exhibit a range of variation. Second, the measuring system may induce variations due to calibration or data acquisition equipment. Random errors may accumulate in a system and produce a variation that must be examined in relation to the quantity being measured.

Defining the tendon design strength in is based on the following statistical analysis. From test data the mean strength and the standard deviation is calculated. The design strength is then set as the mean value less some factor of the standard deviation. Japanese researchers have suggested that the design strength should be set as the mean strength less three standard deviations, which equates to 99.87% inclusion of all test data. This allows the Japanese to specify guaranteed minimum break strength. The FIP and Canadian reports suggest an alternate value of mean strength less 1.65 standard deviations, equal to 95% inclusion. This represents less conservative criterion, yet provides a workable value. A three times standard deviation criteria focuses attention on minimum usable strength, manufacturing quality control, and on simple strand configuration (for instance straight round rods). A 1.65 standard deviation criteria tends to favor innovation and production speed.

Before the standard deviation can be calculated, the number of testing specimens must be defined. The Japanese used a statistical equation to determine the number of tendons that must be tested to achieve statistically valid results and it is shown in Equation 3-1.

$$N = \left(\frac{T \times CV}{\mu} \right)^2 \qquad \textit{(3-1)}$$

The number of specimens to be tested (N) is based on a confidence level to be achieved (T), the percentage of accuracy (μ), and the coefficient of variation of the to be achieved (CV).

The equation is based on results of numerous tests and a 95% confidence interval. The number of specimens used is to be not less than six. This is based on a coefficient of variation of 5.8% and an accuracy of 5% and a confidence value of 1.96 resulting in the following requirement for a minimum of 5.2 test samples:

$$N = \left(\frac{1.96 \times 5.8}{5} \right)^2 = 5.2 \qquad (3\text{-}2)$$

For the testing procedures developed in this project at least six specimens per test condition are required with a method of sampling reported. The procedures outlined in ASTM E 122 cover statistical evaluation of testing.

3.4 References

Castro, P.F., and Carino, N.J. (1997). "Tensile and Nondestructive Testing of FRP Bars." Journal of Composite for Construction, ASCE, Washington, DC, in press.

FIP (1992). High-strength Fiber Composite Tensile Elements for Structural Concrete, FIP Commission on Prestressing Materials and Systems, Institute of Structural Engineers, London, UK, July.

JSCE (1997). "Recommendation for Design and Construction of Reinforced Concrete Structures Using Continuous Fiber Reinforced Materials", JSCE Research Committee, Tokyo, October 1997.

Mandell, J.F., and U. Meier. (1983). "Effects of Stress Ratio Frequency and Loading Time on the Tensile Fatigue of Glass-Reinforced Epoxy," Long Term Behavior of Composites, ASTM STP 813, T.K. O'Brien, ed., American Soc. for Testing and Materials, Philadelphia, PA, pp. 55-77.

Roylance, M. and O. Roylance. (1981). "Effect of Moisture on the Fatigue Resistance of an Aramid-Epoxy Composite," Organic Coatings and Plastics Chemistry, Vol. 45, American Chemical Society, Washington, DC, pp. 784-788.

4.0 STRAWMAN TENDON

Material for this chapter was excerpted from Volume 2 Chapter 1.

Glasforms Corporation of San Jose, CA developed the Strawman tendons specifically for this project. The manufacturer provided individual data on the fibers and resin products used in development of the product. The tendons were manufactured using carbon fiber and an epoxy resin and have the test properties reported in Table 4.1. The rule of mixtures was used to compute the theoretical tendon properties. Using this method produces comparable results to the experimental properties. The average ultimate load that the tendons carried was found to be 96.0 kN (21.6 kips) and the standard deviation is reported with the design capacity. The load versus strain curve is linear as shown in Figure 4.1. The values of the test results are lower than those computed from manufacturer's data for the strength of the tendon. Failure of the tendons occurred when exterior fibers fractured and the tendon lost load.

Table 4.1 - Calculated Strawman Properties versus Average Test Results

	Volume Fraction	Tensile Strength MPa (ksi)	Tensile Capacity kN (kips)	Tensile Modulus GPa (ksi)	Tensile Elongation %
Shell 9405 Resin/9470 Curing agent	35%	64 (9.3)		1.9 (401)	-
T-750 carbon fibers	65%	4480 (650)		165 (34,000)	1.9
Calculated Strawman		2935 (425)	151 (34.0)	108 (22,240)	1.9
Tested Strawman					
Average properties		1862 (270)	96 (21.6)	146 (211,200)	1.2
Standard Deviation, σ		60.7 (8.8)	3.1 (0.70)	2 (310)	0.12
Average –1.65σ			90.9 (20.4)		
Average – 3.0σ			86.7 (19.5)		

The fibers do not yield and do not readily transfer load from the perimeter to the core of the tendon. The differences between calculated and actual tendon performance may be due to the shear-lag between the surface and the core. Working diameter of 8mm approaches the upper bound of tendons size before shear-lag becomes intolerable.
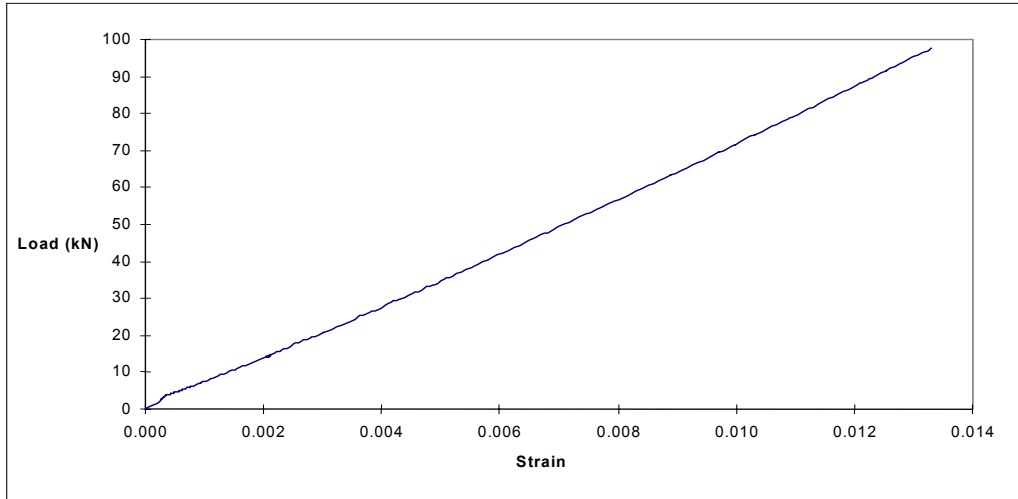
Figure 4.1 - Typical Load-Strain Curve for the Strawman Tendons

5.0 DESIGN SPECIFICATION AND LIMIT STATES

This design specification addresses the following limit states:

- Tendon strength and modulus
- Creep-rupture of FRP tendons,
- Jacking stresses
- Flexural strength,
- Flexural service stresses,
- Axial load and flexure
- Deflection,
- Cracking,
- Fatigue,
- Ductility or deformability,
- Shear, and,
- Bond, development and transfer length requirements.

5.1 General Considerations

Of the limit states above, ductility requires a special explanation. A conventional prestressed concrete beam with a steel tendon will deform elastically until cracking, and then the member deflections will progressively increase as the tendons yield. FRP prestressed beams deform elastically until cracking, then continue to deform under increasing load until the tendon ruptures or ultimate concrete compression strains are exceeded. These two behaviors are compared in Figure 5.1. The intermediate slope in the FRP prestressed beam occurs as the load is increased and the distance from the compression face to the neutral axis of the concrete is reduced, and as the concrete stress- strain behavior becomes non-linear.

Figure 5.1 is based on a beam with over twice the flexural capacity in the steel tendons as in the FRP tendons. This separates the two corves to illustrate the performance differences. The yielding of the steel tendon is evident on the deflection zone of 150 mm to 250 mm (6 in to 10 in). There is no comparable yielding in the CFRP tendons.

Comparison of Harped Prestressing (C1-H, S2)
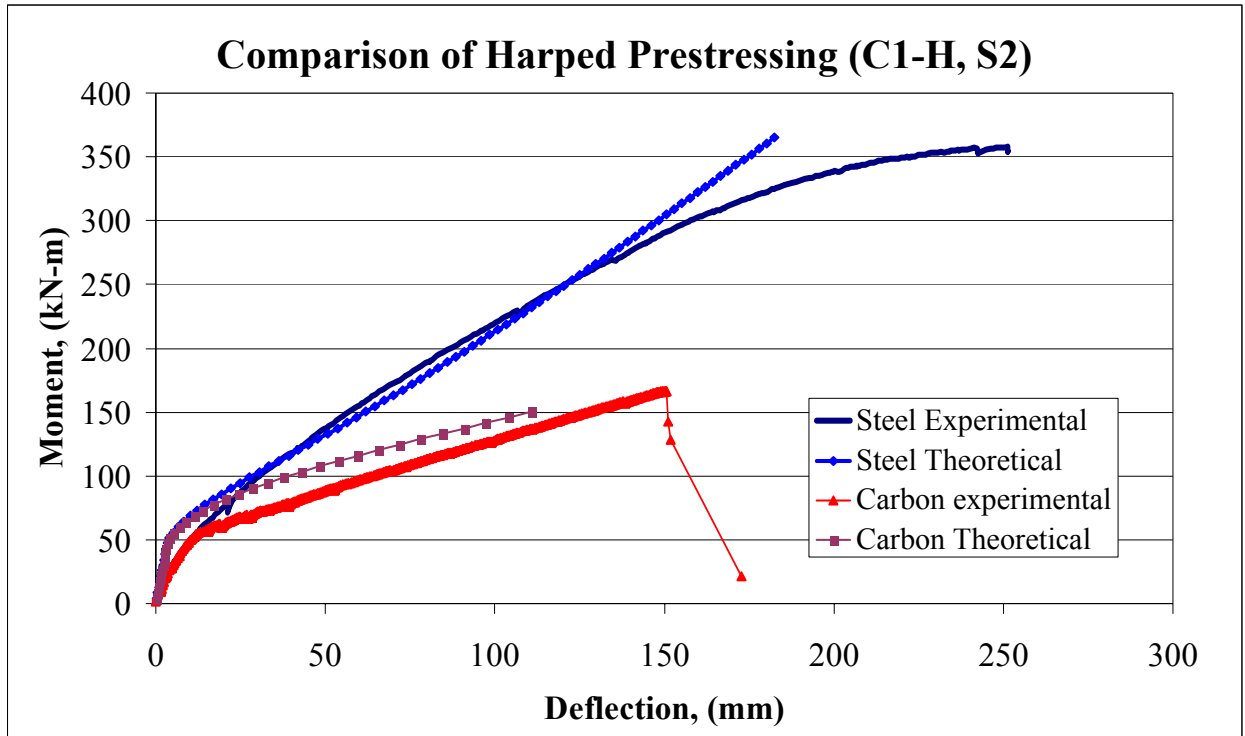
Figure 5.1 Schematic Load-Deflection Curves

The FRP tendon and the concrete are both brittle materials, therefore classical ductility is difficult to obtain. Possible ways to obtain quasi-ductile behavior even with brittle materials are by confining the concrete in compression, partial prestressing, or permitting some bond slip. If ductility is defined as the energy absorbed, then the small area under a FRP prestressed load-deflection curve suggests that energy absorption ductility is very limited [Naaman 1995]. Conversely, ductility may be defined as the ratio of deflection at cracking (or initial yield for steel reinforcement) to ultimate deflection. Using the latter definition as deformability, FRP prestressed members may have considerable deformability. Furthermore, the ability of FRP prestressed members to continue to gain strength with increasing curvature is an inherent safety feature. This capability is more limited with steel prestressing tendons. This is discussed in section 14.

Flexural design limit states include service level stresses and flexural strength requirements. Service level stresses are computed using techniques similar to conventional prestressed concrete. Losses are computed based on elastic shortening, creep and shrinkage of the concrete. Losses for FRP tendons due to these sources are typically less than the

corresponding losses for steel tendons due to the lower modulus of elasticity of the FRP. Relaxation losses are more problematic since there is little data that describes relaxation loss profiles. Relaxation characteristics vary with the fiber type and generally are less than 12 percent over the life of the structure [ACI 440 1996, JSCE 1993]. CFRP tendons have relaxation losses of approximately 5%.

6.0 CREEP-RUPTURE OF FRP TENDONS

6.1 Creep and Creep-Rupture Behavior

Material for this section is excerpted from Volume 2, Chapter 4.

Creep is the inelastic strain of a material under a sustained load over a period of time. Creep-rupture is the tensile fracture of a material subjected to sustained high stress levels over a period of time and occurs when a materials strain capacity is reached. There are three stages of creep: primary, secondary, and tertiary, Figure 6.1. The primary stage, characterized by a continually decreasing strain rate, confined to a short time (relative to creep-rupture time) immediately following application of load in typical polymer matrix composites. The second stage is defined as the time period in which the strain rate is constant under constant stress. In this period some of the weaker strands may fail, but the friction or resin adhesion between the strands transfers the load to adjacent fibers. If the stress level is low enough, fiber damage is confined to the secondary creep level and the tendon has an unlimited service life. The tertiary stage, characterized by an increasing strain rate, represents rapid progressive failure of the fibers until the tendon ruptures.
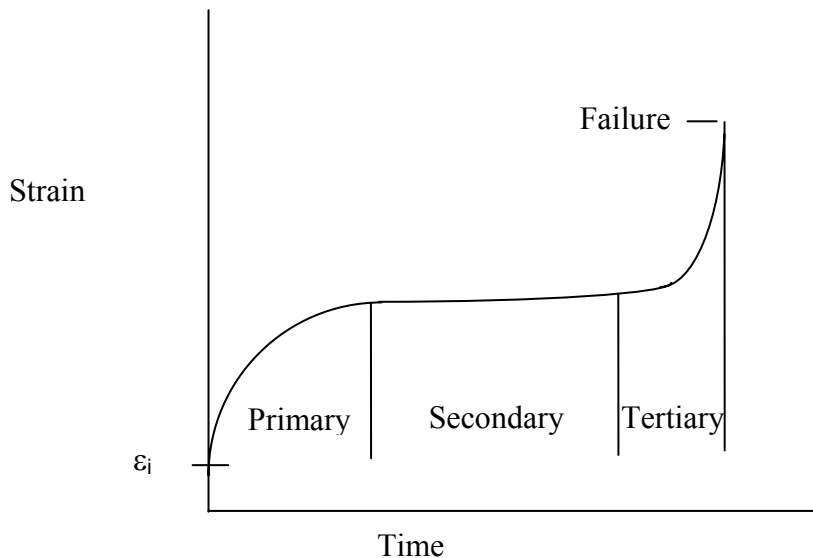
ε_i = initial elastic strain, Load is constant

Figure 6.1 The Three Stages of Creep Deformation

The creep strain relationships of AFRP, GFRP, and CFRP tendons were analyzed under dry conditions [3]. The creep strain behavior of AFRP was typical of the three stages of creep: primary, secondary, and tertiary, Figure 6.1. The GFRP tendon strain increased in steps over a period of time, Figure 6.2. This is likely due to the resolution of the strain measuring equipment. The CFRP tendon showed no secondary creep strain, but rather resulted in instantaneous failure when initial stress levels exceeded the creep-rupture threshold, Figure 6.3
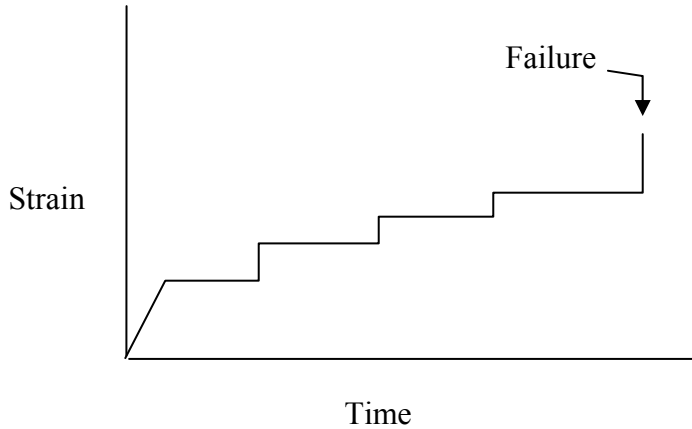
Figure 6.2 Glass Creep-Deformation Curve
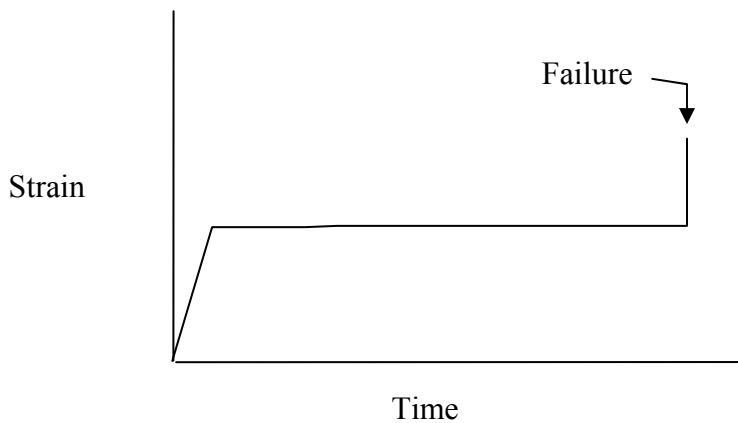
Figure 6.3 Carbon Creep-Rupture Curve

Designers need to know the percentage of ultimate load the tendons may be loaded to so that the tertiary stage is never reached. If the creep in the secondary stage is small, an equilibrium condition will be achieved and the material becomes stable. A full definition of stability in this stage requires an understanding of the individual fiber behavior and the interaction between the fiber and matrix. A probability density function is used to represent creep-rupture times as a function of the applied stress. The Gaussian or Weibull functions, Figure 6.4, were found to be representative density functions. The creep-rupture curve $F_{clm}(t_u)$, in Figure 6.4, is found from static strength test data, short-term creep-rupture data, and long-term creep-rupture data. The static strength distribution is found from a series of ultimate strength tests on a particular material. The short-term and long-term creep-rupture distributions are found from a series of data points representing material failure at a particular applied load, F_{cl}. The creep-rupture curve for a FRP material is formed from the mean failure time, t_s, and a corresponding F_{cl} .
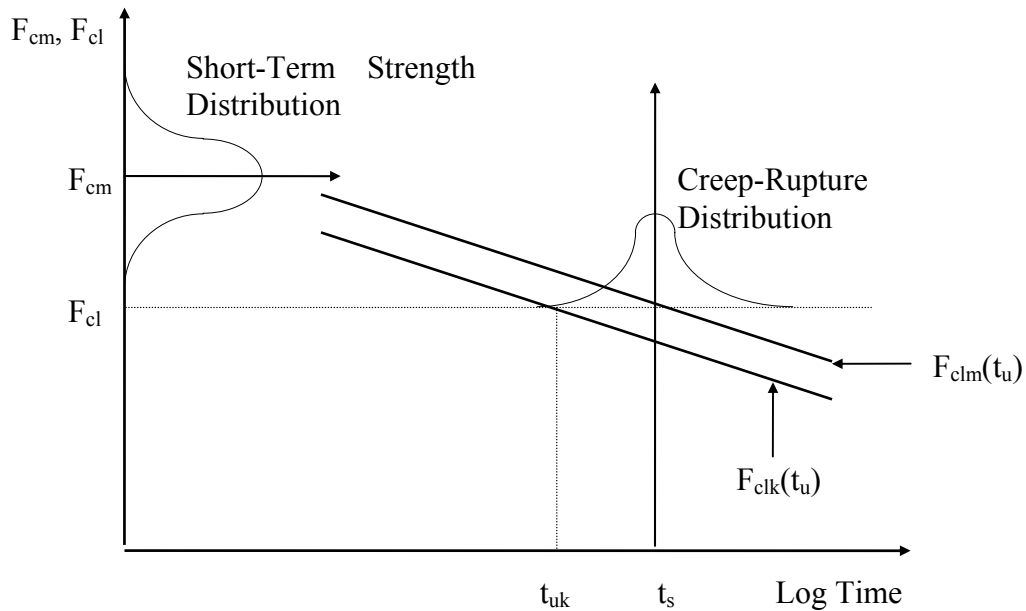
Figure 6.4 Characteristic and Mean Creep-Rupture Curves for FRP Tendons

(Adapted from Rostasy 1993)

Notation: $F_{clk}(t_u) =$ Characteristic endurance, a function of t_u
$\qquad\qquad F_{clm}(t_u) =$ Mean endurance, a function of t_u
$\qquad\qquad F_{cl} =$ Constant sustained load less than the static capacity
$\qquad\qquad F_{cm} =$ Mean of sustained loads less than the static capacity
$\qquad\qquad t_s =$ Mean failure time
$\qquad\qquad t_{uk} =$ Characteristic failure time
$\qquad\qquad t_u =$ time variable

Two methods are employed to obtain creep-rupture data, opening loaded frames and constant load frames. Each method has its advantages and disabilities. Each method is described as below. Creep-rupture tests are run for tendons in the 50-80 percent of ultimate load range. Above 90% of ultimate, data is collected with a load control universal machine.

6.2 Spring Loaded Testing Frame

Testing establishes the creep-rupture response corresponding to 50–80 percent of static strength and to observe the effects of the saltwater and concrete environment on the creep behavior of the FRP tendons. The spring load reduces slightly due to creep of the tendon and anchor slip. This reduction in load is comparable to the loss of prestress in a concrete structure. Desired tensile loads were achieved by using coil springs and a 3 m (10 ft) tall, I-beam, test frame, Figure 6.4, 6.5. Positioning the linearly-tapered epoxy-socked anchor between the beam flanges creates a safe method of testing the long-term strength of the tendons. The anchor is coupled to a threaded rod that serves to transfer the load due to the compressed spring. Test specimens were placed in the frame and one anchor was filled with epoxy and permitted to cure. After the anchor had cured the specimen was removed and placed in the bottom of the frame so that the second anchor could be cast-in-place. The concrete core was cast around the tendon using paper forms. The paper form was stripped after the initial concrete curing. An environmental chamber was placed around the tendon/concrete combination and was sealed. The tendon was loaded by compressing the spring using a loading frame and hydraulic jack. The spring's displacement indicates the amount of force exerted on the tendon. When the tendon ruptures, the frame restrains the spring and anchor assembly.

Front View   Side View
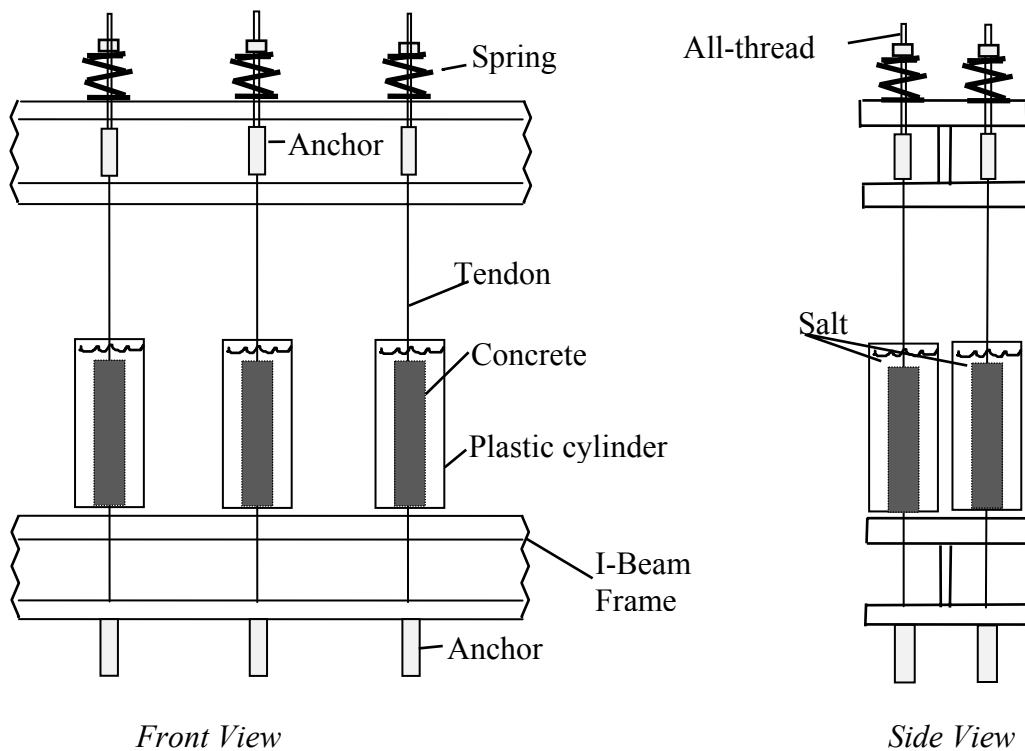
Figure 6.4 Long-Term Creep-Rupture Spring Loaded Test Frame Assembly

6.3 Constant Load Test frames

A constant load test frame uses a cantilever arm and a weight to establish a constant load on the tendon. The cantilever arm rotates as the tendon creeps. This requires careful detailing of the anchor tendon assembly to prevent kinking of the tendon at the anchor and corresponding false readings in the time to failure.

Figure 6.5 Spring Loaded Test Frames with Epoxy Anchors and Environmental Chamber

6.4 Conclusions of Creep-Rupture Testing

Creep-rupture tests were conducted for over 12,000 hours. At the conclusion of the tests, unbroken tendons were removed and tested for residual strength. Strength decay data was then extrapolated to 1,000,000 hours. Figure 6.5 shows the carbon tendon results. The extrapolation through the 12,000-hour points is very conservative because tendons did not fail. A more moderate prediction places the extrapolation below the residual strength and the stress at 12,000 hours. Figure 6.6 indicates the final extrapolations for aramid, carbon and glass fiber tendons.

The epoxy plug within the epoxy anchors relaxes over time and becomes wedged tighter into the tapered core of the anchor. The epoxy plug slides axially in the direction of load compressing the neoprene grommet. The relaxation within the epoxy anchor due to these factors allows the spring to decompress, which decreases the sustained load on the specimen. After a period of time, equilibrium is reached between anchor relaxation and sustained load loss. The calculated loss in the applied load from the beginning to the end of this test program was between 10–15 percent. The loss in load is the reason for the missing data points in the range of 70–85 percent F_u for the three creep-rupture curves. The combination of anchor relaxation and material creep contributed to excessive axial movement of the anchor/tendon assembly. The top anchor of some test specimen came into contact with the top flange of the frame and data was adjusted. The use of expansive cement anchors with test specimen loaded in the spring loaded test frame was one method used to remedy the load relaxation problem. The long-term creep-rupture tests conducted on Carbon T-300 FRP rods use expansive cement anchors and are tested in the spring-loaded frame to fill in the missing creep-rupture data for CFRP.

The 10-15% reduction in residual strength for CFRP and AFRP tendons due to environmental exposure of these tests indicates that the service life environments degrade the tendons. The low residual strength results for the CFRP and AFRP environmental portions are due, in part, to the concrete removal procedure. The 6-7% reduction in residual strength values for CFRP and AFRP air-exposed portions is most likely due to failure initiation caused by the epoxy anchors attached to one end of the specimen. Many of the specimen failures appeared to originate near the epoxy anchors. The effects of fiber straightening should increase the strength of the tendon as in other residual strength tests.

The creep-rupture curves provide predicted allowable prestress loads for AFRP, CFRP, and GFRP rods for any given service life. The predicted stress level for CFRP is 0.70 F_u for 100 years of service. Additionally, the long-term residual strength of CFRP is 0.90 F_u. The upper limit of service load at a 100-year life for AFRP is predicted to be 0.55 F_u in a concrete environment and the long-term residual strength of AFRP is 0.80 F_u. Predicted stress levels for GFRP rods for a 100-year service life are 0.40 F_u in a dry environment. GFRP appeared to be especially susceptible to damage due to solution cycling. The solution cycling was delayed for a period of four months during the summer to simulate a dry season. At the onset of the solution cycling (~8,000 hrs) the remaining specimen failed within a two-month period.

6.5 References

Rostasy F.S. & M. Scheibe (1995). "Stress-Rupture of AFRP Subjected to Alkaline Solutions and Elevated Temperature – Experiments." <u>Non-metallic Reinforcement for Concrete Structures</u>. E & FN Spon, London, UK.

ASTM D 2990, (1995)"Standard Test Methods for Tensile, Compressive, and Flexural Creep and Creep-Rupture of Plastics," ASTM D 2990 – 93a, ASTM, West Conshohocken, PA.

$K = -2.0598\text{Ln}(t) + 84.878$

$K = -2.3839\text{Ln}(t) + 80.089$

% Load Ratio, K

Time, hours

Legend:
- ◆ CR Failure
- ■ No Failure
- ✕ Mean Envir. Exposed Res. Strength
- ✱ Mean Air Exposed Res. Strength
- — Log. (CR Failure)
- — Log. (Predicted)
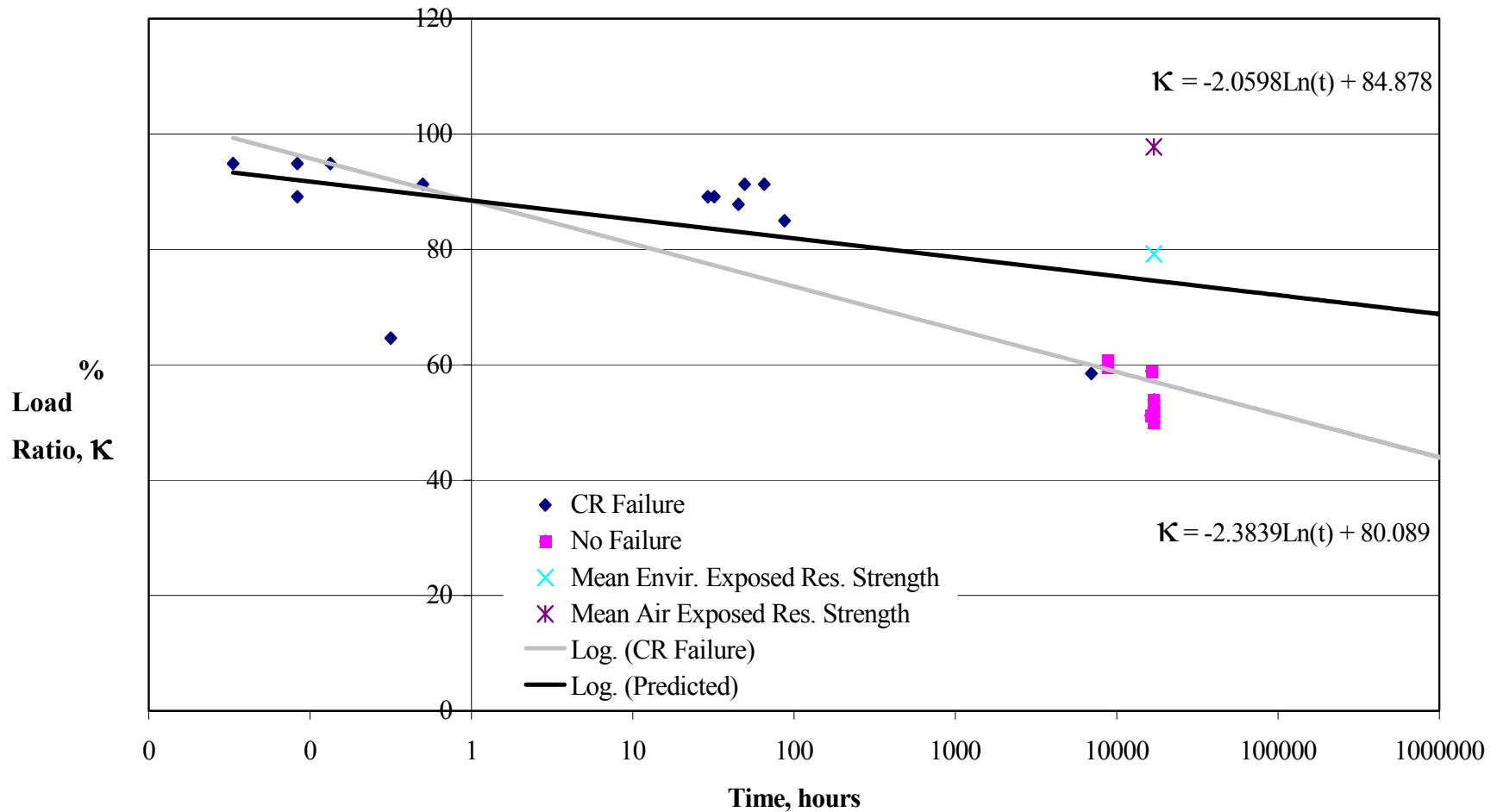
Figure 6.5 Actual and Predicted* Creep-Rupture Curves for Carbon T-600 FRP Rods Under Environmental Exposure, Including Mean Residual Strengths**
*"Log. (Predicted)" Curve Excludes the "No Failure" Data Points
**All Tests except Residual Strength Tests used Epoxy Anchors. Anchor Failures not Included.
Residual Strength Tests used Expansive Cement Anchors
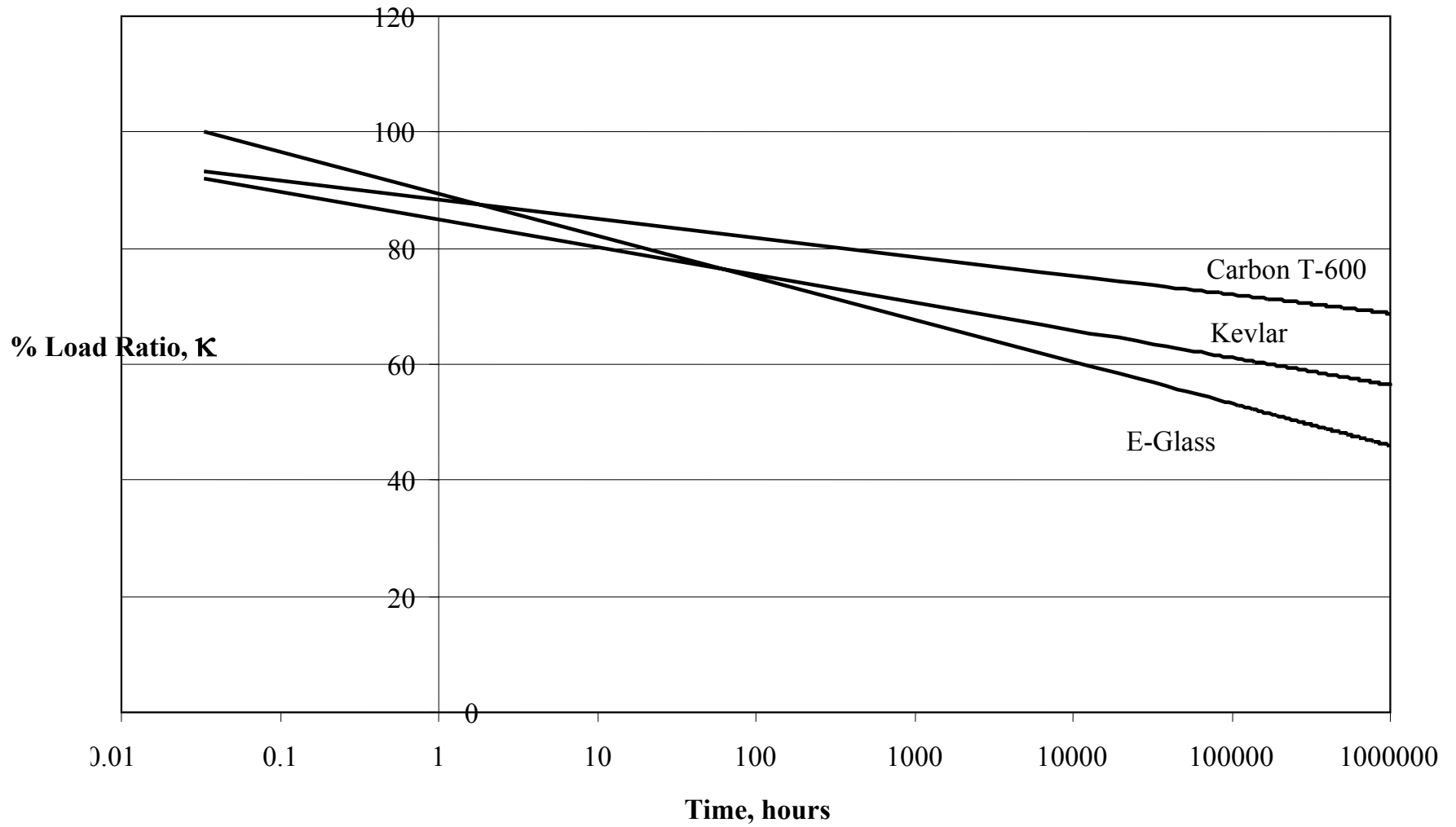
Figure 8.1 Comparison of Creep-Rupture Curves for E-Glass, Kevlar, and Carbon T-600 FRP Rods Under Environmental Exposure

7.0 JACKING STRESSES AND LOSSES

The tendon jacking stress and losses are dependent upon the material characteristics of the tendon. This section presents the overall recommendations for jacking stresses for straight tendons. The chapter then provides corrections to those stresses for harped tendons and corrections for relaxation of CFRP tendons.

7.1 Allowable Jacking Stresses

Based on the creep-rupture tests described in Section 6, the recommended maximum jacking stresses for straight FRP tendons are given in Table 7.1. Overstressing FRP tendon can reduce the service life because the stresses are higher on the creep-rupture curves. Stresses for jacking and for immediately following transfer are provided so that the tendon may be compensated for any anchorage loss. Overstressing for relaxation is not recommended because it results in a higher long-term strain on the fibers.

Table 7.1 Allowable Tendon Stresses

Allowable Jacking Stresses		Pretensioned	Post-tensioned
	Carbon	$0.65\,f_{pu}$	$0.65\,f_{pu}$
	Aramid	$0.50\,f_{pu}$	$0.50\,f_{pu}$
	Glass	Not recommended	$0.45\,f_{pu}$
Allowable stress immediately following transfer			
	Carbon	$0.60\,f_{pu}$	$0.60\,f_{pu}$
	Aramid	$0.40\,f_{pu}$	$0.40\,f_{pu}$
	Glass	Not recommended	$0.40\,f_{pu}$

The stress-corrosion of glass due to alkali reaction makes it unsuitable for prestressing applications when the glass is in contact with the concrete. Values are given for glass in post-tensioning applications where the designer can assure that the glass is isolated from the alkali in the cement.

7.2 Corrections for harped tendons

FRP tendons have no ductility. Therefore, the jacking stresses must be reduced to account for stress increases when a tendon is bent over a fixed radius harping point. The stress increase in the tendon is given by equation 7-1.

$$\sigma_h = \frac{E_f y}{R} \qquad (7\text{-}1)$$

where E_f is the modulus of elasticity of the FRP tendon, y is the distance from the centroid of the tendon to the tensile face, and R is the radius of curvature of the harping saddle.

Equation 7-1 is correct for solid tendons and is conservative for stranded tendons. The individual "wires" in a stranded tendon will have less effective curvature than a comparable solid rod. Equation 7-1 also provides guidance for the design of harping saddles. As seen in Chapter 13, the fatigue tests were conducted with a 0.9 m (36 in) radius for the harping saddle in order to control the total tendon stress.

The combined stress in the tendon must be less than the values provided in Table 7.1. Therefore the combined stress in a tendon of cross sectional area, A_f, at a harping saddle due to the jacking load, P_j, is given computed from equation 7-2.

$$\sigma = \frac{P_j}{A_f} + \frac{E_f y}{R} \qquad (7\text{-}2)$$

7.3 Relaxation Losses

Relaxation losses in FRP tendons derive from three sources. First, when the tendon is initially stressed, a portion of the load is carried in the resin matrix. Second, the fibers in a pultruded section are nearly, but not completely parallel. Third the fibers themselves relax. Over time, the matrix relaxes and looses its contribution to the load carrying capacity, R_1. Stressed fibers flow through the matrix and straighten. This straightening appears as a relaxation loss, R_2. Thirdly, the fibers themselves are prone to relaxation, R_3. These three effects may be assessed separately and the total relaxation is $R = R_1 + R_2 + R_3$.

The initial matrix relaxation occurs in the first 24 to 96 hours and may be accelerated by heat curing of prestressed concrete beams. Two characteristics of the tendon affect this relaxation, the volume of fibers in the tendon, v_f, and the modular ratio of the resin to the fiber. For an elastic modulus of the resin, E_r, and a modulus of the fiber, E_f, the modular ratio of the resin, n_r, is given in equation 7-3.

$$n_r = E_r/E_f \qquad (7\text{-}3)$$

For resins used in pultrusion operations, the modular ratio ranges between 1.5 to 3% for carbon and aramid fibers. The lower values are for carbon and the higher for aramid. The relaxation loss is the product of the volume fraction of the resin, $v_r = 1-v_f$, times the modular ratio. Therefore the initial relaxation loss, R_1, is given by equation 7-4.

$$R_1 = n_r \times v_r \qquad (7\text{-}4)$$

The resin volume fraction is typically 35 to 40 percent of the tendon cross section. Therefore, the total relaxation in the first phase is 0.6 to 1.2 percent of the transfer stress. Overstressing for this loss is possible providing the total stress limits in table 7.1 are not exceeded. Overstressing and allowing the relaxation to reduce the stress to the values in Table 7.1 is not recommended because the loss does not occur in the fibers and the fibers would be permanently overstressed.

Straightening of the fibers is a function of the quality control of the pultrusion process. The packing of the fibers in a solid pultrusion precludes much straightening. A one to two percent relaxation is adequate to predict this phase of loss calculation. Thus, $R_2 = 0.02$.

Fiber relaxation is dependent upon the fiber type. Carbon fibers are reported to have no relaxation. High stress level creep-rupture tests have confirmed this behavior. Therefore, R_3 for carbon may be assumed to be zero. Aramids have a creep behavior that is reflected in their relaxation behavior. The Dupont data book suggests that the long-term relaxation of Kevlar fibers is 1 to 3 percent per decade on a log scale. Assuming that the relaxation count begins after the first 24 hours, the total relaxation for aramids

may be assumed to be 6 to 18 percent in a 100-year design life. Thus R_3 is zero for carbon and up to 18 percent for aramids.

7.4 Other Losses

Other losses traditionally associated with prestressing tendons, such as initial elastic shortening and concrete creep and shrinkage, are computed in the same manner as for steel tendons. The modulus of elasticity of the FRP tendon is typically lower than a corresponding steel tendon. Therefore, the magnitude of these losses will be less than the corresponding steel losses.

8.0 FLEXURAL DESIGN

Material for this section is excerpted from Volume 2, Chapters 2 and 3.

Numerous flexural tests of FRP prestressed members are reported in the literature. Comprehensive testing began in the mid 1980's in Japan with carbon and aramid tendons and in Europe with aramid and glass tendons [Gerritse 1991]. The first tests in the USA were conducted on aramid tendons and reported by Dolan [Dolan 1990]. In the intervening years, several attempts have been made to combine these data into design or performance recommendations [FIP 1992, JSCE 1992]. The lack of uniform testing protocols and consistent reporting procedures made completion of these criteria very difficult.

8.1 Strength Design Methodology

The approach to strength design of FRP prestressed beams is based on the concept of a brittle ratio, the reinforcement ratio that simultaneously results in failure of the tendons and the concrete. Concrete failure is taken as an extreme compression strain of $\epsilon_{cu} = 0.003$. This strain limit assumes no allowance is made for confinement of concrete due to the presence of closed stirrups or other auxiliary confinement. A rectangular stress block is used to model the concrete behavior. Tendon failure is defined as the ultimate tensile strain of the tendons, ϵ_{pu}. Having defined the brittle ratio, design conditions for members with reinforcement ratios above and below the brittle ratio are developed.

8.2 Brittle Ratio

Figure 8.1 defines the cross-section, strain and stress conditions for the condition where the tendon ruptures simultaneously with the compression failure of the concrete.
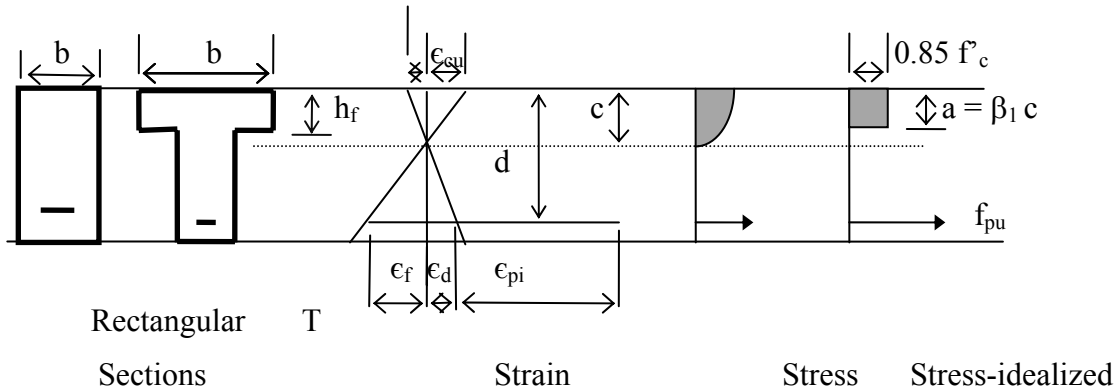
Figure 8.1: Brittle Ratio - Stress and Strain Conditions

The derivation is for a rectangular section or a T-section where the compression block is within the depth of the flange, that is, $a < h_f$. This analysis uses only a single layer of reinforcement.

If the total strain capacity of the tendon is denoted ϵ_{pu}, then the amount of strain available for flexure, ϵ_f, is the total strain less the amount used for prestressing, ϵ_{pi}, the strain used to decompress the compression zone, ϵ_d, and any loss of strain capacity due to sustained loads, ϵ_{pr}. This relationship is given in equation 8-1.

$$\epsilon_f = \epsilon_{pu} - \epsilon_{pi} - \epsilon_d - \epsilon_{pr} \tag{8-1}$$

The strain compatibility from Figure 8.1, allows determination of the c/d ratio in terms of the available strains. Therefore, by using similar triangles:

$$\frac{c}{d} = \frac{\varepsilon_{cu}}{\varepsilon_{cu} + \varepsilon_{pu} - \varepsilon_{pi} - \varepsilon_d - \varepsilon_{pr}} \tag{8-2}$$

Equilibrium on the cross section equates the tensile force of the tendon to the compressive force on the concrete. Hence, (8-3)

$$0.85 f_c' \beta_1 cb = \rho_{br} bd f_{pu} \tag{8-3}$$

Solving for ρ_{br} gives

$$\rho_{br} = 0.85 \beta_1 \frac{f_c'}{f_{pu}} \frac{c}{d} \tag{8-4}$$

Substituting in the expression for c/d from equation 8-2 gives the brittle ratio in the form of material properties.

$$\rho_{br} = 0.85 \beta_1 \frac{f_c'}{f_{pu}} \frac{\varepsilon_{cu}}{\varepsilon_{cu} + \varepsilon_{pu} - \varepsilon_{pi} - \varepsilon_d - \varepsilon_{pr}} \tag{8-5}$$

An examination of the various strain components leads to simplification of the brittle ratio equation. First, the strain loss due to sustained loads is nearly zero if the sustained load is less than 50% of the ultimate tensile strain. This condition is typically satisfied because the prestress strain is 50% of the ultimate strain in order to leave some capacity for flexural strain. Secondly, the decompression strain, ϵ_d, is typically an order of magnitude less than the flexural strain. Setting these two strain values to zero gives the following simplified definition for ρ_{br}.

$$\rho_{br} = 0.85 \beta_1 \frac{f_c'}{f_{pu}} \frac{\varepsilon_{cu}}{\varepsilon_{cu} + \varepsilon_{pu} - \varepsilon_{pi}} \tag{8-6}$$

The tendon strain ϵ_{pu} - ϵ_{pi} is the residual strain available for flexure. FRP tendons have ultimate strains ranging from 1.2% to 6.0%. Compared to the yield stress of normal steel reinforcement, there is substantial strain capacity available to allow the flexural

member to deform and crack prior to failure. This provides visual warning of overload conditions.

In a typical design project, ϵ_{pi} is known because the designer selects it. The manufacturer provides the ultimate stress and strain for the tendon. The designer does need to know the basis for the selection of these values. For example, some manufacturers provide the mean stress and strain while Japanese manufacturers typically provide a value equal to the mean less three standard deviations. Eventually the industry will establish a standard for reporting that is consistent with the capacity reduction factors for FRP tendons.

8.3 Flexural Design and Capacity Prediction

The flexural behavior of beams may be divided into three groups. If $\rho > \rho_{br}$, the beam will fail by compression of the concrete with no failure of the tendon. For beams with a reinforcement ratio between $0.5\ \rho_{br}$ and ρ_{br}, the tendon will rupture and the concrete compressive stresses will be substantially non-linear. For this case an equivalent rectangular stress distribution can be used to predict beam strength. If $\rho < 0.5\ \rho_{br}$ then the beam is significantly under-reinforced and the concrete stress approaches a linear condition. The nominal moment capacity for each of these conditions is developed below.

Normal Beam Reinforcement- $0.5\ \rho_{br} \leq \rho \leq \rho_{br}$

For this condition, the compression force is equal to the tensile force, which is established by the size and ultimate tensile strength of the tendon. The selection of 0.5

ρ_{br} as the delineating point for this equation is selected on the basis of concrete behavior. Further confirmation with experimental results is required to validate this limit. Summing moments about the compression centroid defines the nominal moment capacity as:

$$M_n = \rho \ bdf_{pu}(d - \frac{a}{2}) \qquad\qquad (8\text{-}7)$$

where a is computed from equilibrium on the cross section.

$$a = \frac{\rho \ d \ f_{pu}}{0.85 \ f_c'} \qquad\qquad (8\text{-}8)$$

Combining the value for **a** with the nominal moment equation provides a combined form for prediction of nominal moment capacity. If the prestressing tendons are not in a single layer, the nominal capacity is reduced as discussed later.

$$M_n = \rho \ bd^2 f_{pu}(1 - \frac{\rho}{1.7} \frac{f_{pu}}{f_c'}) \qquad\qquad (8\text{-}9)$$

Under-reinforced Beam - $\rho \leq 0.5 \ \rho_{br}$

For very lightly prestressed beams the full non-linear capacity of the concrete compression block does not develop and a linear stress strain distribution more correctly represents the stress condition in the member. The determination of the value of the reinforcement ratio for this to occur will depend upon experimental validation, but is taken as $\rho < 0.5 \ \rho_{br}$ for this discussion. The solution for this condition is the same as for working stress design of reinforced concrete beams. The neutral axis is established by setting the first moment of area of the section equal to zero. For a linear concrete stress

strain distribution, the distance from the compression face to the neutral axis is defined as c = kd. The solution for k is given in texts on reinforced concrete (Nilson 1991) and repeated in equation (8-10).

$$k = \sqrt{(\rho n)^2 + 2\rho n} - \rho n \qquad (8\text{-}10)$$

Where ρ is the reinforcement ratio and **n** is the ratio of the modulus of elasticity of the tendons to that of concrete. The nominal moment may be computed by summing the moments about the compression centroid. The centroid is that of a triangle and is located one third of the depth of the compression block below the compression face. The nominal moment capacity for an under-reinforced beam is then:

$$M_n = \rho \ bd^2 f_{pu} \left(1 - \frac{k}{3}\right) \qquad (8\text{-}11)$$

Over-reinforced Beam - $\rho \geq \rho_{br}$

In an over-reinforced beam the concrete will fail in compression prior to the failure of the tendon. The stress and strain compatibility is the same as in Figure 8-1; however, the value of the tendon strain is not known. The solution to this condition is to locate a neutral axis compatible with an elastic tendon. This is done by defining the strain in the tendon, equilibrating the horizontal forces on the section, solving for the neutral axis location, and finally summing moments about the tendon. First, the neutral axis location is defined as $c = k_u d$. The strain in the prestressing tendon is equal to the initial prestress, ϵ_{pi}, plus the flexural strain ϵ_f. The latter can be computed by proportional strain knowing the ultimate concrete strain, ϵ_{cu}.

$$\varepsilon_p = \varepsilon_{pi} + \varepsilon_{cu} \frac{1 - k_u}{k_u} \tag{8-12}$$

The tendon stress is $f_p = \epsilon_p E_p$, and equilibrium on the cross section is

$$\rho \, bdf_p = 0.85 f_c' b \beta_1 k_u d \tag{8-13}$$

substituting in values for strain and elastic modulus gives:

$$\rho \left(\varepsilon_{pi} + \varepsilon_{cu} \frac{1 - k_u}{k_u} \right) E_p = 0.85 f_c' \beta_1 k_u \tag{8-14}$$

Defining a materials constant λ, such that

$$\lambda = \frac{E_p \varepsilon_{cu}}{0.85 f_c' \beta_1} \tag{8-15}$$

and substituting equation 15 into equation 14 allows the resulting quadratic equation to be solved for k_u.

$$k_u = \sqrt{\rho \, \lambda + \left(\rho \, \lambda \left(1 - \frac{\varepsilon_{pi}}{\varepsilon_{cu}} \right) \right)^2} - \frac{\rho \, \lambda}{2} \left(1 - \frac{\varepsilon_{pi}}{\varepsilon_{cu}} \right) \tag{8-16}$$

As before, the depth of the compression block is $a = \beta_1 c = \beta_1 k_u d$. Summing moments about the tendon gives the nominal moment capacity of an over-reinforced beam.

$$M_n = 0.85 f_c' b \beta_1 k_u d^2 \left(1 - \frac{\beta_1 k_u}{2} \right) \tag{8-17}$$

8.4 Development of Flexural Capacity for Vertically Distributed Tendons

The above derivations assume that the prestressing tendons are all located at the same depth from the compression face. To analyze vertically distributed tendons a method for determining the strength of vertically aligned CFRP tendons is presented. The method is based on an elastic analysis and the strain distribution shown in Figure 8.2. The analysis is developed for a T-section with the assumption that the neutral axis is in the flange. Strain due to decompression is fairly small and has been neglected. Strain due to elastic and non-elastic shortening of the section are neglected as these strains are regained at the maximum curvature.
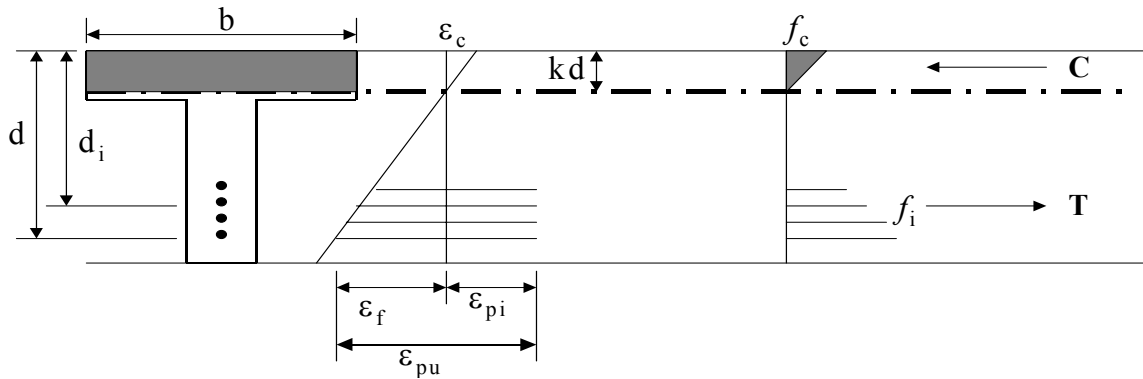
Figure 8-2 Cracked Elastic Section with Vertically Distributed Tendons

Define $f_m = f_{pu} - f_{pi}$ as the flexural failure stress of the bottom tendon that is remaining after the initial prestress. The stress in each tendon can be defined by a ratio of the strain at any level to the strain in the bottom tendon.

$$f_i = f_{pi} + f_m \frac{d_i - kd}{d - kd} = f_{pi} + f_m \left(\frac{\frac{d_i}{d} - k}{1 - k} \right) \qquad (8-19)$$

where d_i is the depth of each individual tendon, d is the depth of the bottom tendon, and kd is the location of the neutral axis in a cracked section. The neutral axis for beams with varying depth tendons is given as follows:

Define the initial prestress ratio, $\xi = \dfrac{f_{pi}}{f_{pu}}$, and ρ_i is the reinforcement ratio at each level, then:

$$k = \frac{\sqrt{\left(n\sum_{i=1}^{m}\rho_i\right)^2 + 2(1-\xi)n\sum_{i=1}^{m}\rho_i\left(\xi + \dfrac{d_i}{d}(1-\xi)\right)} - n\sum_{i=1}^{m}\rho_i}{1-\xi} \qquad (8\text{-}20)$$

Let $\psi_i = \dfrac{d_i}{d}$ the depth ratio of the tendons. If all of the tendons are prestressed to the same initial prestress, then the moment capacity for uniformly prestressed tendons is

$$M_n = bd^2\sum_{i=1}^{m}\rho_i f_i\left(\psi_i - \frac{k}{3}\right) \qquad (18\text{-}21)$$

If the tendons are individually prestressed to account for the vertical distribution of strain due to the distribution of tendons through the depth of the member, then the nominal moment capacity is given as:

$$M_n = bd^2\sum_{i=1}^{m}\left\{\rho_i\left[\left(f_{pi} + f_m\left(\frac{\psi_i - k}{1-k}\right)\right)\left(\psi_i - \frac{k}{3}\right)\right]\right\} \qquad (8\text{-}22)$$

Most beams have a relatively small number of levels of prestress. Therefore, equation 21 and 22 are readily solved on a spreadsheet. The full derivation and details of assumptions are given in Volume 2.

8.5 Design Implications of Vertically Distributed Tendons

Equations 8-21 and 8-22 provide a means to optimize the design of FRP prestressed beams. The prestressing ratio, ξ, may be varied at each depth so that the final stress distribution in the tendons is uniform with depth at maximum curvature. The reinforcement ratio may also be varied with depth to account for beams with mixed strand patterns such as harped strands and a large number of straight strands in the bottom flange.

8.6 Recommended Phi Factors for Flexure

A survey of all flexural tests reported in the literature was conducted and the ratio of experimental strength was compared to the strength predicted by the equations in this chapter. The comparison allows a determination of the capacity reduction factor based on either the type of tendon or the type of failure. Both ratios are given in Table 8.1. The capacity reduction factor is based on material and sectional properties rather than on the type of failure. Therefore, capacity reduction factors for aramid and carbon tendons are presented in table 8.2. The recommended capacity reduction factors are based on normalizing the mean strength to the predicted strength for a β value of 1.65. The carbon tendons make this objective. The aramid tendons do not quite reach this goal, in part due to the difficulty of establishing the actual strength of the aramid tendons from the literature.

Table 8.1 Comparisons of Experimental and Theoretical Strength

| | | $\dfrac{M_{exp}}{\phi M_n}$ | | | | | |
		Ratio $\phi=1.00$	Ratio $\phi=0.90$	Ratio $\phi=0.85$	Ratio $\phi=0.80$	Ratio $\phi=0.75$	Ratio $\phi=0.70$
All Beams	Mean	1.097	1.219	1/366	1.371	1.462	1.567
	Std. Dev.	0.196	0.218	0.221	0.245	0.261	0.280
	β for mean $-\beta\sigma =$	0.494	1.004	1.259	1.514	1.769	2.024
(30 samples)	1.0						
Under reinforced beams	Mean	1.161	1.290	1.366	1.452	1.548	1.659
	Std. Dev.	0.188	0.209	0.221	0.235	0.251	0.272
	β for mean $-\beta\sigma =$	0.857	1.388	1.654	1.920	2.185	2.451
(14 samples)	1.0						
Over reinforced beams	Mean	1.040	1.156	1.244	1.300	1.387	1.486
	Std. Dev.	0.190	0.212	0.244	0.238	0.254	0.272
	β for mean $-\beta\sigma =$	0.212	0.737	0.999	1.262	1.524	1.787
(16 samples)	1.0						
Aramid tendons	Mean	1.021	1.135	1.202	1.277	1.362	1.459
	Std. Dev.	0.237	0.263	0.278	0.296	0.316	0.338
	β for mean $-\beta\sigma =$	0.091	0.513	0.725	0.936	1.147	1.358
(8 samples)	1.0						
Carbon Tendons	Mean	1.149	1.277	1.352	1.437	1.532	1.642
	Std. Dev.	0.178	0.198	0.209	0.222	0.237	0.254
	β for mean $-\beta\sigma =$	0.840	1.403	1.684	1.965	2.247	2.528
(19 samples)	1.0						

Table 8.2 Recommended Capacity Reduction Factors.

Tendon type	Capacity Reduction Factor, ϕ
Aramid	0.70
Carbon	0.85
Over-reinforced beams	0.70
Under-reinforced beams	0.85

8.7 References

Dolan, C. W. (1990). "Developments in Non-Metallic Prestressing Tendons". PCI JOURNAL, Precast/Prestressed Concrete Institute, Chicago, IL, Vol. 35, No. 5, September p. 80.

Gerritse, A. and Werner, J., (1991) "ARAPREE - a non-metallic tendon," Advanced Composite Materials in Civil Engineering Structures, ASCE, materials Engineering Division, New York, NY, pp. 143-154.

FIP (1992). High-strength Fiber Composite Tensile Elements for Structural Concrete, FIP Commission on Prestressing Materials and Systems, Institute of Structural Engineers, London, UK, July.

JSCE (1992). "Application of Continuous Fiber Reinforcing Materials to concrete Structures," Concrete Library International, No. 19, Japan Society of Civil Engineers, Tokyo, p. 89.

9.0 FLEXURAL SERVICE STRESSES

Concrete service load stresses remain the same as specified by AASHTO and are given in Table 9.1.

Table 9.1 Allowable Concrete Stresses

Allowable stresses at transfer of prestress (prior to losses)	
(a) Extreme fiber stress in compression	$0.60 \, f_{ci}'$
(b) Extreme fiber stress in tension except for (c)	$3\sqrt{f_{ci}'}$
(c) Extreme fiber stress in tension at ends	$6\sqrt{f_{ci}'}$
Allowable stresses under service loads (following losses)	
(a) Extreme fiber stress in compression due to prestress plus sustained loads	$0.45 \, f_c'$
(b) Extreme fiber stress in compression due to prestress plus total loads	$0.60 \, f_c'$
(c) Extreme fiber stress in precompressed tensile zone	$6\sqrt{f_c'}$
(d) Extreme fiber stress in tension due to prestress plus short duration loads	0

10.0 PILE DRIVING AND IN SITU FLEXURE

Material for this section is excerpted from Volume 3, Section C.

10. 1 General

The axial performance of precast concrete piles prestressed with FRP was evaluated. The piles were 6.1 m (20 ft) in length and had a 0.3 m by 0.3 m (12 in by 12 in) cross-section. They were prestressed using carbon FRP rods. The spiral reinforcement was also fabricated using CFRP. One pile was tested at the laboratory to evaluate flexural performance. The second pile was driven in the field to evaluate axial performance and then tested in flexure. The results of the flexural tests were then compared with one another. Two additional piles with similar cross-section but prestressed with steel tendons rather than CFRP rods were also constructed. One of these was tested in the lab to verify flexural performance. The other was driven in the field alongside the CFRP prestressed pile to act as a reaction for the flexural test.

10. 2 CFRP Spirals Manufacturing

The fabrication of the two sections of CFRP spiral served two purposes. The first was to evaluate the use of CFRP spirals as a confinement material for axially loaded members. The second purpose was to evaluate the manufacturing process and is beyond the scope of this report. The spirals were made of Zoltek Panex 33-0048 fibers and Shell Epon Resin. The fibers have a 3.62 GPa (525 ksi) guaranteed tensile strength. Two identical sections of spiral were fabricated, one for each of the two piles. Each spiral section has 21 turns (five turns at 25 mm (1 in) pitch and 16 turns at 75 mm (3 in) pitch) for a total length of 1.325 m (53 in). The spiral sections were installed at one end of the piles, which would later be the end in contact with the ram in the case of the driven pile. The rest of the pile section was confined with conventional steel spirals, Figure 10.1.

The manufacturing technique for the confinement spirals is described below with the aid of photographs. A strand of carbon fibers consisting of ten 48K fiber tows (20 mm^2 (0.031 in^2) cross-sectional area) was held together and pulled through a resin bath for impregnation. Once the fibers were fully impregnated, the strand was pulled through

a circular dye to remove extra resin. After that, the impregnated strand was wrapped on a mandrel of appropriate diameter, Figure 10.2. Finally, the spirals were cured on the mandrel at room temperature for 24 hours.
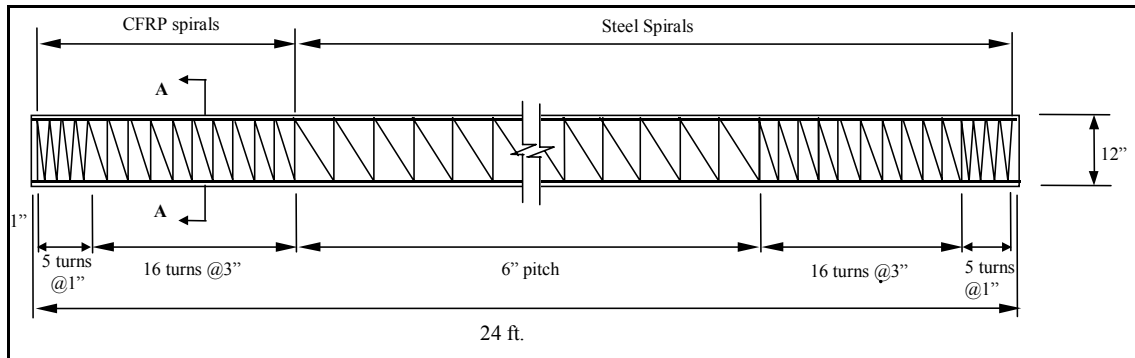
Figure 10.1 Spiral Reinforcement Configuration (1-in = 25.4 mm)
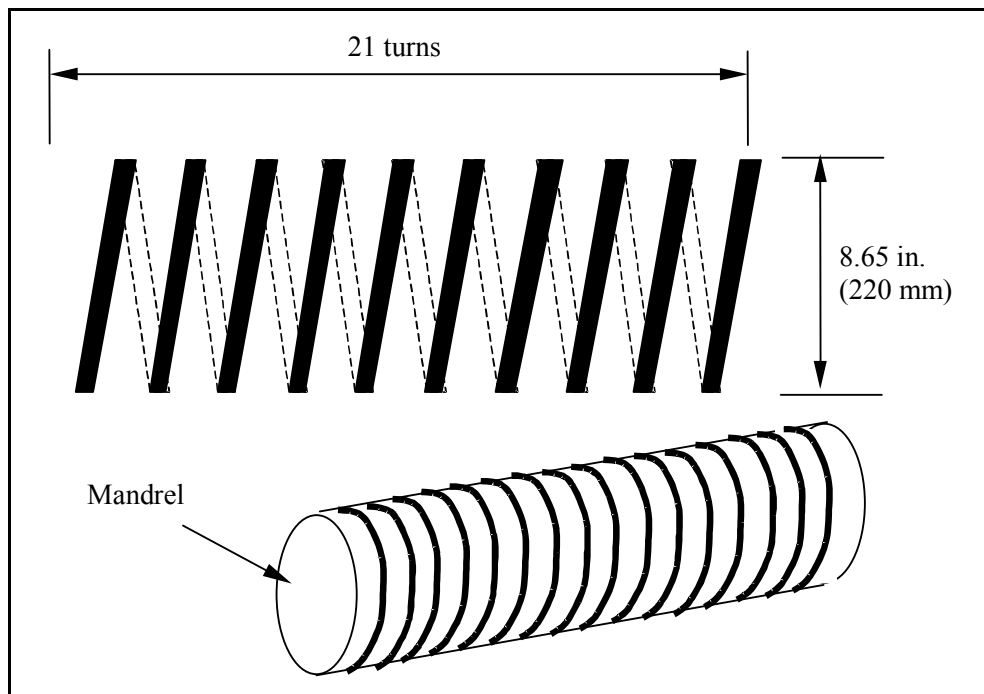
Figure 10.2 Details of CFRP Spirals

10. 3 Pile Flexural Test Program

The first pile was tested in flexure in a four-point loading scheme. The actual loaded span length 5.62 m (18 ft). Deflections were recorded at the supports, quarter-

span, and mid-span. Compression strain measurements were collected at mid-span. Horizontal deflection was recorded in both the compression and tensile zone of the cross-section to develop a moment-curvature relationship.

The pile displayed small deflection up until cracking. Once the cross-section had cracked and the section stiffness was reduced and a much greater degree of deformability was observed. The section recovered deflection well when unloaded. This elastic behavior continued until failure of the beam. An audible warning to failure was heard when the tendons started to lose their bond with the cross-section. No-slip of the tendons at the section ends was observed however. Failure of the section was obvious and sudden. A loud "pop" was heard accompanied by a sharp decrease in the load at the moment of the first tendon failure.

Failure in the section resulted from rupture of the FRP tendons. The moment-curvature diagram displays the characteristic bi-linear response with two ascending branches and a decrease in stiffness after cracking. Cracking of the section occurred at approximately 37.3 kN-m (330 kip-in) and the ultimate moment was approximately 76.8 kN-m (680 kip-in). The calculated moment due to the self-weight of the beam is included in the moment-curvature diagram for accuracy as well as comparison purposes. In the field test, the pile is tested in a vertical configuration thereby eliminating any effects due to the weight of the beam. The moment-curvature diagram is given in Figure 10.3. The load-deflection diagram shows a corresponding behavior and is seen in Figure 10.4.
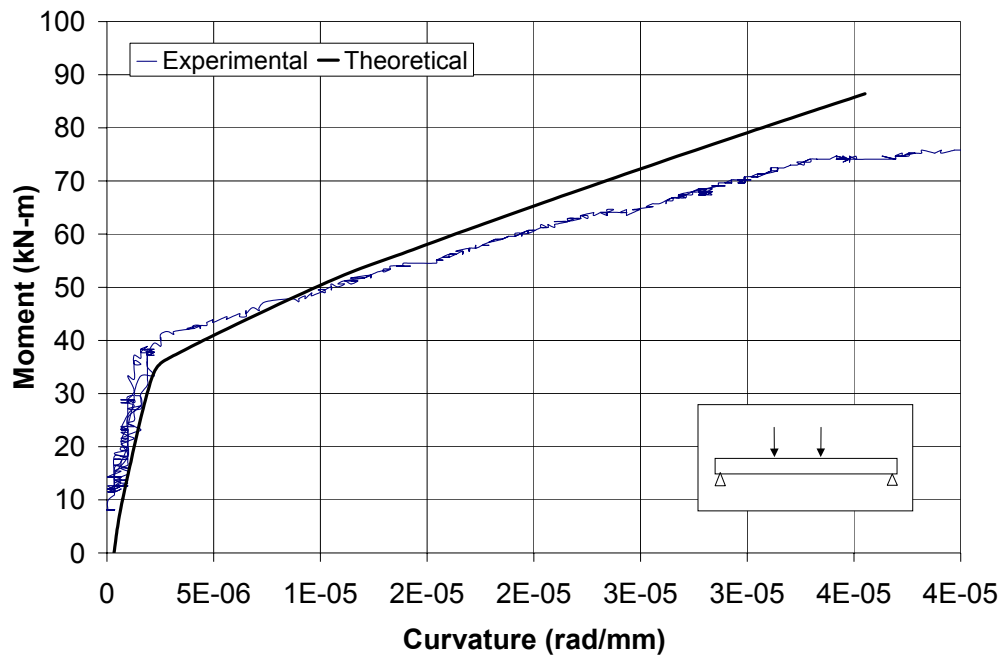
Figure 10.3 Moment-Curvature Relationship (1-in = 25.4-mm, 1-kip = 4.448-kN)
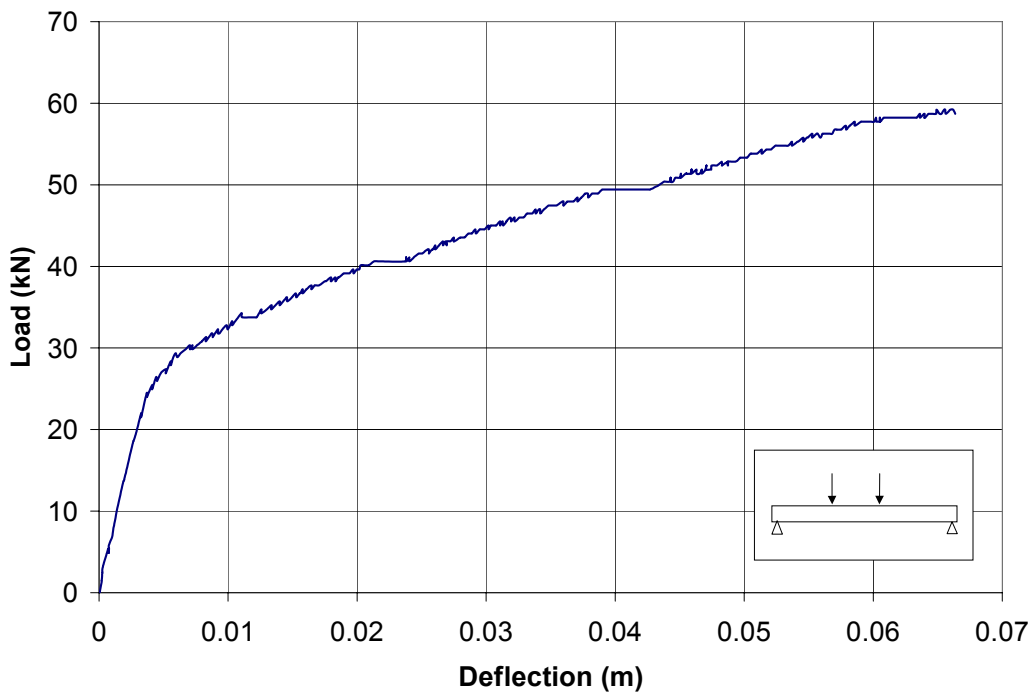
Figure 10.4: Load-Deflection Envelope for Pile Lab Test (1-in = 25.4-mm, 1-kip = 4.448-kN)

10.4 Axial Performance Evaluation

10.4.1 Driving FRP Prestressed Piles in the Field

To prepare for the driving process the piles needed to have a tapered end cast onto them. Standard concrete piles in use have a driving tip that helps to prevent twisting or displacement when an obstacle is encountered during the driving. The driving tips were anchored to the piles through four threaded anchor bolts that were doweled into the pile section.

Two piles were transported to a construction site and driven in the field. One pile was prestressed with FRP tendon and the other with steel tendons. The steel pile was to be used as a reaction for the static load test described later. The piles were driven with a Kobe K-13 single-acting diesel hammer with a weight of 12.8 kN (2870 lbs.) Figure 10.5. Extra care was taken in the placement of the piles before driving in order to protect the instrumentation that was in place at the time. The piles were driven into a rocky-clay fill material on the approach to a new bridge. Neither pile was driven to bedrock. Once the pile was driven the pile head was inspected for damage. Aside from some minor chipping at the square edges no damage was observed.

Figure 10.5 Driving of Pile Section

10.4.2 Field Test Setup

A jack was suspended from above the piles to allow loading at a point 0.5 m (1.5 ft) from the top of the piles (see Figure 10.6). The piles were restrained against horizontal displacement near ground elevation through the use of high-strength steel rods and small spreader beams. Load readings were recorded at the point of load application and at the restraint. Deflections were measured at the point of loading, at the restraint and midway between the two. Rotation was measured at the base. Strains were measured at several locations. Compression strains were measured using 50 mm (2 in) strain gauges on the compression face of the section. Tensile strains were measured through extensometers, or clip-gauges, on the tensile side of the section. Strains were also monitored in the tendons on the tensile side of the section.

Figure 10.6 Photo of Field Static Load Test

10.4.3 Field Test Results

The testing in the field displayed similar results to that performed in the lab. Once the hydraulic jack was engaged to the cross-section care was taken not to drop the load below 4.5 kN (1000 lbs). The first crack observed in the cross-section occurred at ground level. The next crack occurred at the location of the instrumentation. Once this

crack had propagated a knife-edge on one of the extensometer was caught rendering the gauge ineffective. Another minor problem during the testing was the fact that some of the LVDTs would stick after unloading requiring them to be freed.

The cross-section displayed an elastic behavior up to failure for this test as well as the lab control sample. Once cracking of the cross-section had occurred the section displayed greater deformability due to the reduced stiffness. Failure was very similar to the laboratory test, displaying the same audible warnings followed by a loud "pop" and a sharp decrease in the load.

Comparing the moment-curvature relationship of the two tested piles to the analytical moment-curvature shows a close match. The maximum moment of the laboratory tested pile section was about 12.3 percent lower than the theoretical maximum moment. The pile tested in the field showed even closer results, with a maximum moment only 7.5 percent below the theoretical.
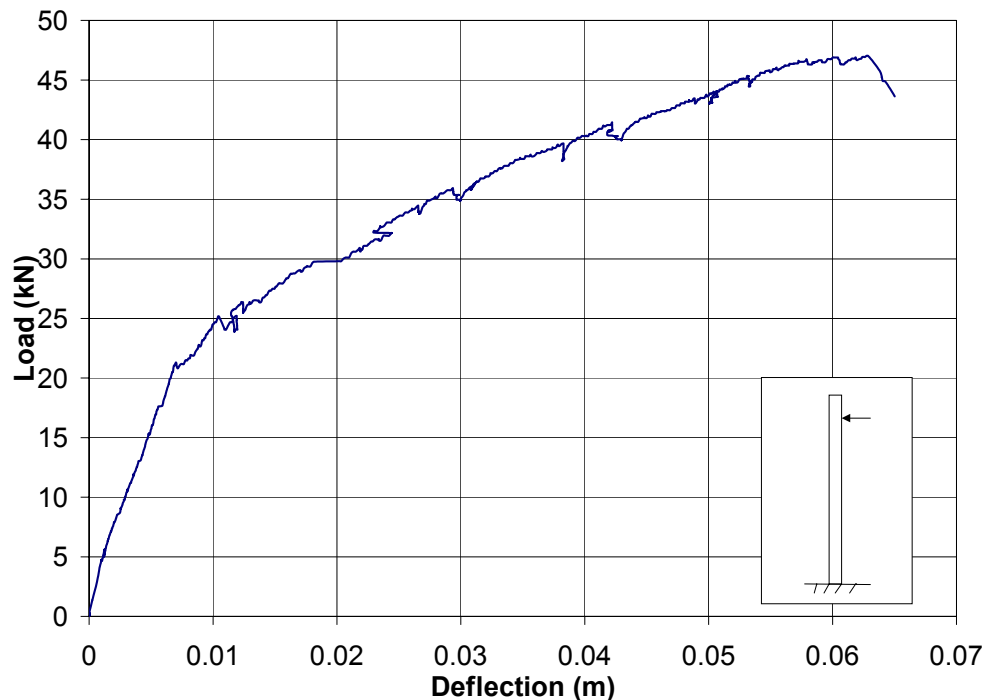
Figure 10.7 Load-Deflection Envelope at Point of Loading

(1-in = 25.4-mm, 1-kip = 4.448-kN)

10.5 CONCLUSIONS

The results of the flexural test performed in the field were in close agreement with results obtained from the laboratory-controlled test indicating little or no effect on bond of tendons due to the driving of the piles. The CFRP spirals performed adequately in this application, though the pile was driven neither to bedrock or rejection.

Though this project shows that it is possible to manufacture PC members using CFRP tendons there is still much work to be done before this becomes a feasible application. A more standard approach needs to be developed for anchorage work as well as better control over tendon manufacturing. The presence of defects in the tendons can be detrimental to the prestressing procedures itself. These issues need to be addressed before prestressing can become a more viable alternative to conventional prestressing.

11.0 DEFLECTION

Material for this section is excerpted from Volume 2, Chapter 11.

11.1 Short-term deflection

Deflections for FRP prestressed beams are be divided into two categories: short-term and long-term deflections. Deflection of beams prestressed by FRP tendons can be determined based on modified effective moment of inertia, I_e proposed by ACI Committee 435 (1995) as given by equation (11-1). Prior to cracking, the gross moment of inertia can be used to calculate the deflections from traditional mechanics of materials. Following crack formation, methods need to be utilized that take into account the softening effect that cracking has on concrete members. This can be accomplished through the following equation:

$$I_{eff} = \left(\frac{M_{cr}}{M}\right)^3 I_g + \left(1 - \left(\frac{M_{cr}}{M}\right)^3\right) I_{cr} \tag{11-1}$$

where I_{eff} is the effective moment of inertia, I_g is the gross moment of inertia, M_{cr} is the cracking moment, and I_{cr} is the cracked moment of inertia, which can be calculated with the following equation.

$$I_{cr} = \frac{b(kd)^3}{3} + nA_{ps}(d - kd)^2 \tag{11-2}$$

In equation 11-2, the depth to the neutral axis is computed the same as for reinforced concrete if the reinforcement is in a single layer, equation 8-10. If the prestressing is distributed vertically through the section, k is found from equation 8-20 and n is the modular ratio for the FRP tendon shown in equation (11-3).

$$n = \frac{E_f}{E_c} \tag{11-3}$$

Most of the load deflection data examined indicated that the above approach is valid for loads between cracking of the concrete and up to 50 percent of the ultimate load. Beyond the range of 50 percent of the nominal moment capacity, the above

calculations are stiffer than the actual section. This is due to the assumption that the section remains elastic and the actual beam compression zone is softer than the elastic assumption. Abdelrahamen has suggested modifications to this approach that more accurately predict the behavior of the beams in his test series. (Abdelrahman 1999) Beams with the tendons distributed vertically through the depth of the section displayed slightly more deflection than predicted by the methods of ACI 435.

Deflection due to specified live load should be calculated as the difference between the deflection due to the total service load and the deflection due to dead load. This is not only due to the change of the effective moment of inertia, I_e, but also due to the change of the eccentricity of the prestressing force after cracking.

11.2 Long-Term Deflections

Long-term deflections were not within the scope of this project but research is available on the subject (Currier 1995). For long-term deflections, camber and deflection are separated into individual components, adjusted by a modifier, and then superimposed to obtain final deflections. Current modifiers recommended by PCI are shown in Table 11.1 for flexural beam members within a recommended span to depth ratio of 10 to 20, as recommended by the PCI Design Handbook (PCI Section 3.2.2). The revised modifiers developed by Currier for predicting long-term deflections by the PCI Design Handbook method are as shown in Table 11.2. These modifiers are for members without composite toppings. The modifier for each tendon was developed under a philosophy to leave the deflections due to self-weight and dead loads constant.

Table 11.1. PCI Design Handbook Multipliers for Deflection (PCI Section 4.6.5)

	Without Topping	*With Topping*
At erection:		
(1) Deflection (downward) component-apply to the elastic deflection due to the member weight at release of prestress	1.85	1.85
(2) Camber (upward) component apply to the elastic camber due to prestress at the time of release of prestress	1.80	1.80
Final:		
(3) Deflection (downward) component-apply to the elastic deflection due to the member weight at release of prestress	2.70	2.40
(4) Camber (upward) component-apply to the elastic comber due to prestress at the time of release of prestress	2.45	2.20
(5) Deflection (downward) apply to elastic deflection due to superimposed dead load only	3.00	3.00
(6) Deflection (downward)- apply to elastic deflection caused by the composite topping	----	2.30

Table 11.2. Suggested PCI Modifiers for FRP Tendons.

		Without Composite Topping			
		Steel	CFCC	Aramid	E-Glass
At Erection:	*Deflection due to self-weight.*	1.85	1.85	1.85	1.85
	Camber due to prestress	1.80	1.80	2.00	1.70
Final:	*Deflection due to self-weight*	2.70	2.70	2.70	2.70
	Camber due prestress	2.45	0.00	0.00	0.75
	Deflection due to applied loads	3.00	4.10	4.00	3.00

11.3 References

Branson, D.E. and Trost, H. (1982) "Unified Procedures for Predicting the Deflection and Centroidal Axis Location of Partially Cracked Non prestressed and Prestressed concrete Members", ACI Structural Journal, V. 79, No. 2, 119-13 0.

Abdelrahman, A.A., and Rizkalla, S.H. (1997) "Serviceability of Concrete Beams Prestressed by Carbon Fibre Reinforced Plastic Bars", ACI Structural Journal, Vol. 94,

No. 4, 447-457.

Abdelrahman, A. A., and Sami H. Rizkalla, (1999) "Deflection Control of Concrete Beams Pretensioned by CFRP Reinforcements", Journal of Composites for Construction, Vol. 3, No. 2.

12.0 CRACKING

Material for this section is excerpted from Volume 2, Chapters 3 and 7.

12.1 Crack Widths

The crack widths were observed and recorded during flexural testing of FRP Prestressed girders. Crack widths were also recorded during cycles of fatigue. Placement for the linear potentiometers was determined after first cracks were identified and at the completion of the first one million cycles of the beam. Linear potentiometers were placed where cracks were observed nearest the harp point, Figure 12.1.
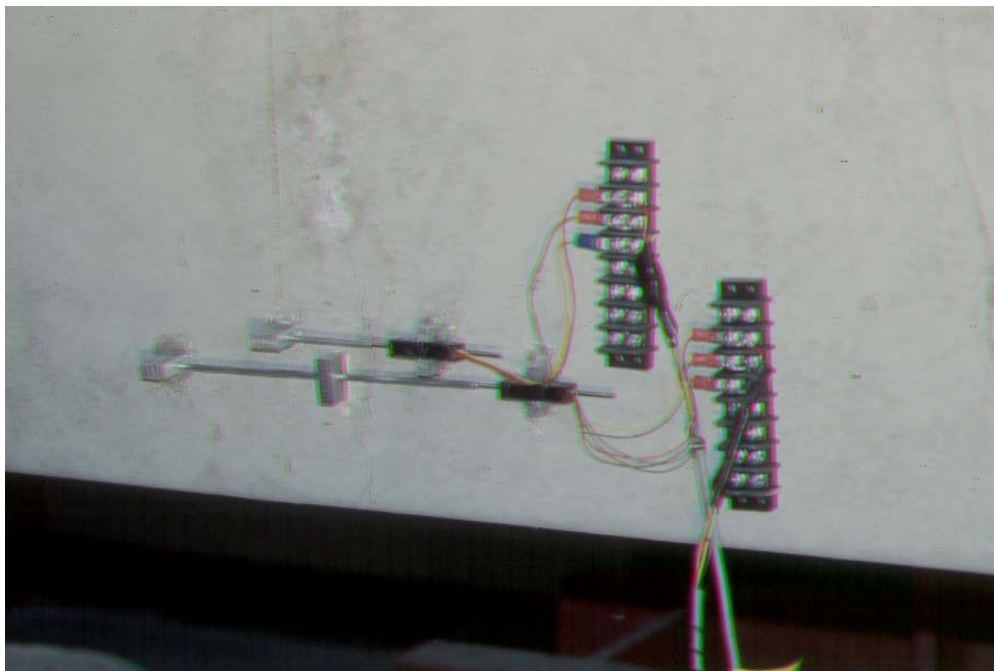
Figure 12.1 Setup of Linear Potentiometers

Figure 12.2 shows the variation of crack width versus tendon stress for each reinforcing material. Linear trends are seen for both carbon and steel once the initial precompression is overcome. Crack spacing for the different beams did not vary significantly. The cracks were evenly spaced at about 250 mm (10 in.) suggesting major debonding of the carbon tendons did not occur during static or fatigue loading.
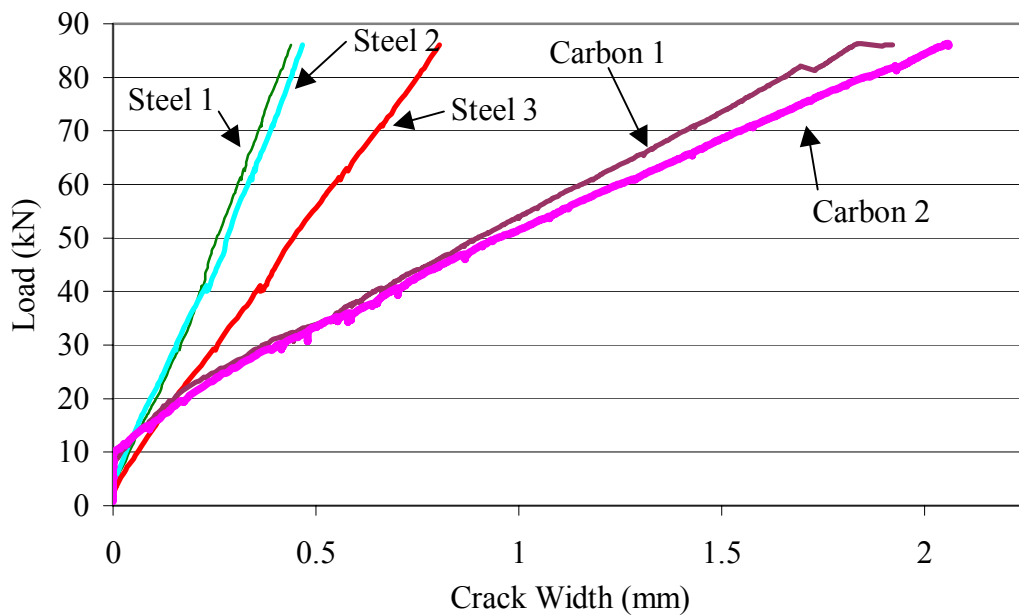
Figure 12.2 Carbon and Steel Crack Widths during Ultimate Strength Static Test

Crack width may be reasonably predicted using the Gergely-Lutz crack width equation. The crack width prediction must be adjusted by the modulus of ratio of the steel to the FRP tendon. Thus, the crack width for beams with FRP tendons is:

$$w_{frp[} = w_{steel}\frac{E_s}{E_f} \tag{12-1}$$

where w_{frp} is the crack width on thousands of an inch and w_{steel} is the predicted crack width based on the original Gergely-Lutz formulation.

13.0 FATIGUE

Material for this section is excerpted from Volume 2, Chapters 3 and 7.

13.1 Fatigue Life

Two beams prestressed with steel and carbon tendons respectively were tested for conditions then monotonically loaded to failure fatigue. The beams were cracked at the first load of P_{max}. The steel and carbon prestressed beams survived 3,000,000 cycles without showing any fatigue failure due to a nominal tensile stress of up to $0.5\sqrt{f_c^{'}}$ MPa ($6\sqrt{f_c^{'}}$ ksi) at the beams most extreme fiber. Gradual softening of the girders was observed, but the beams indicated no loss of strength due to the fatigue loadings.

13.2 Fatigue Evaluation

The load-deflection curves for the final monotonic flexural capacity for the carbon and steel prestressed beams after 3,000,000 cycles of loading are shown in Figure 13.1. The strength of the girders exceeded the predicted capacity by four percent for the carbon girder and one percent for the steel girder. Concrete cover at the critical section, the crack position at failure, was removed and the carbon tendons were carefully inspected. The saddle for the harping point was also extracted and inspected for signs of fatigue friction and fretting of the tendons, Figure 13.2. The failed tendons are shown in Figure 13.3.
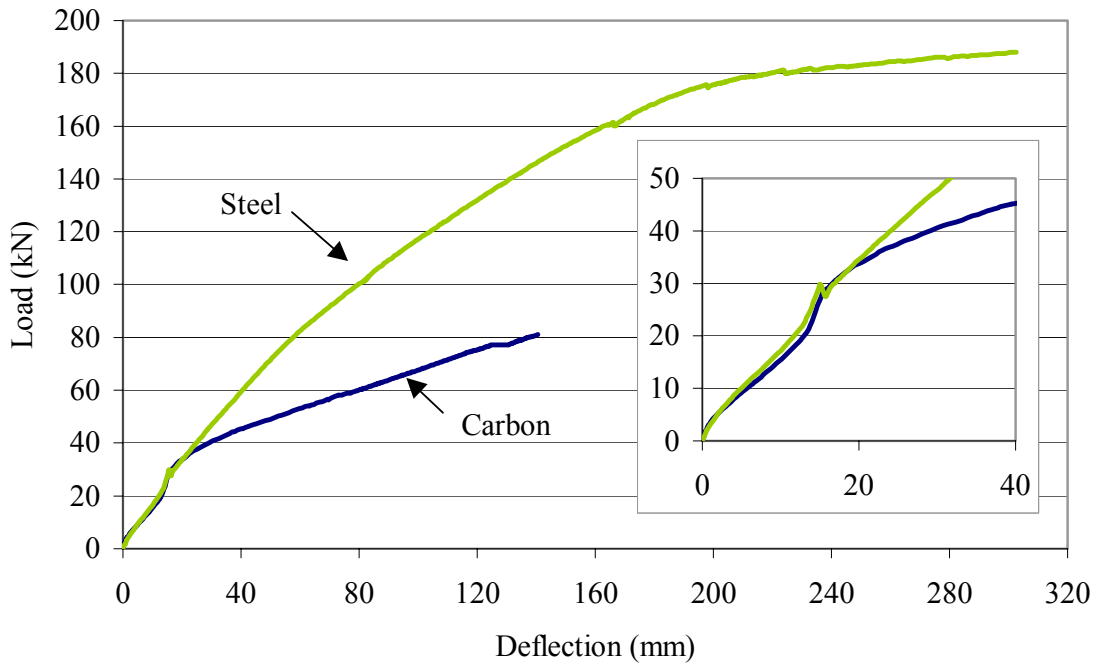
Figure 13.1 Ultimate Load-Deflection Plot after 3,000,000 cycles
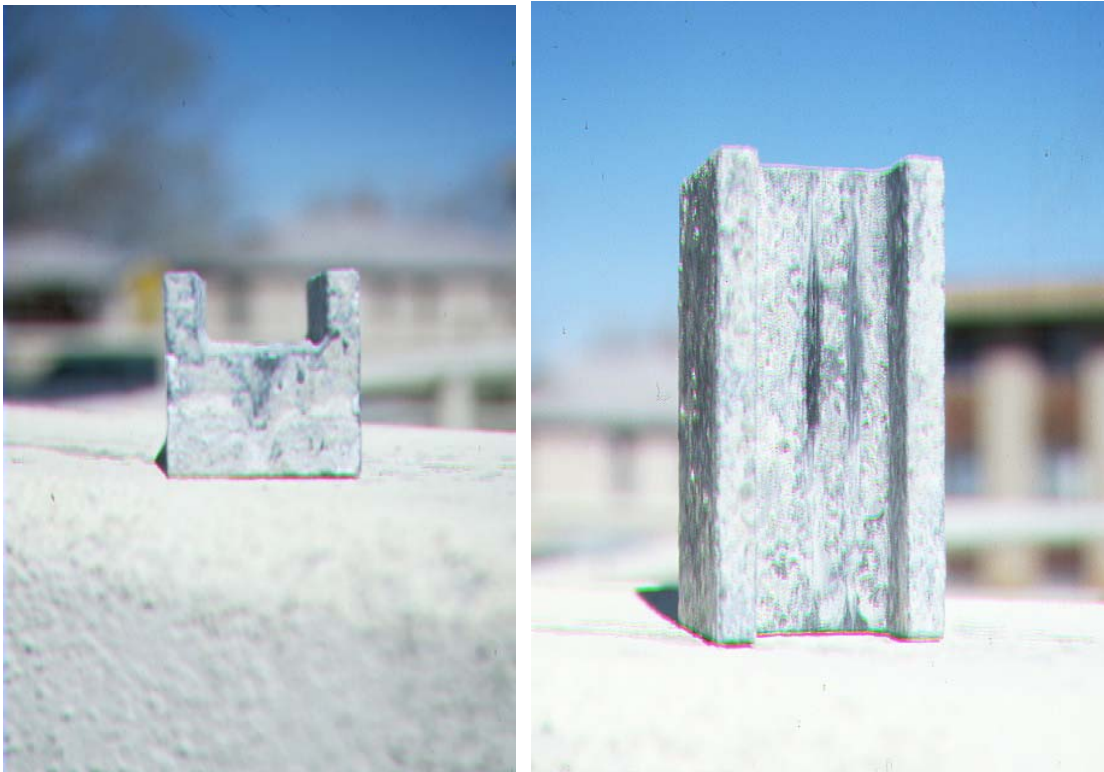
Figure 13.2 Friction Evidence on Saddle

Figure 13.3 Carbon Tendons After Failure

The failed tendons were typical of a tensile failure were best explained as a straw broom failure. Since all the carbon tendons failed in tension at close to the predicted strength, it can be assumed that full tensile strength of the tendon was developed. The saddle had evidence of some sliding contact between the tendons and the saddle during fatigue, Figure 13.2. However, no significant fraying of the tendons was visible. There was evidence of contact near the edge of the saddle. It is recommended that a small radius be turned on the edges of any production saddle to minimize possible edge or bending effects.

The reason for the difference in the magnitude of the nominal moment capacity of the carbon and steel reinforced prestressed girders is a result of the difference in total area of reinforcement. A design objective was to place the same number of strands in each beam to keep the same geometry and harping configuration in the two girders. Had

a 3/8 in, Grade 270 steel stand been available instead of the ½ in, Grade 270 steel strand the beams would have had more comparable moment capacity. This would have allowed a better comparison for the ultimate capacity of the carbon girder to the steel girder. Using the ½ in. steel strand assured that the stress levels in the steel were below the recommendations of ACI 215 for fatigue breaking (ACI Committee 215 1997).

Crack Width

Figure 13.4 shows the crack pattern in the constant moment section of the carbon tendon girder. The initial static test created a well-developed tendon series of flexural cracks for the carbon girder. Similar results were observed in the steel girder. The average crack spacing was 230 mm to 305 mm (9 to 12 in.), which approximately coincided with the stirrup spacing of 254 mm (10 in.). Crack lengths for the initial static load are indicated by dots placed on the crack pattern. Cycling caused some new cracks to form and some to extend. Even distribution of cracks after the static test and the continued even distribution of cracking during the fatigue cycling suggest sufficient bond was available. Overall, bond is considered good and localized bond deterioration is limited. A section of concrete was collected from the test beams to show that deformations in the tendon helped the bond between the concrete and the tendon.

Crack widths increased slightly due to fatigue loading. Several major crack widths were read during each intermediate static load test. A plot of these measured crack widths versus number of cycles is shown in Figure 13.5. During the final static load test the cracks continued into the top of the flange of the girder. Shear was neither computed to be significant nor a cause of any of the cracks observed.

Applied Loads
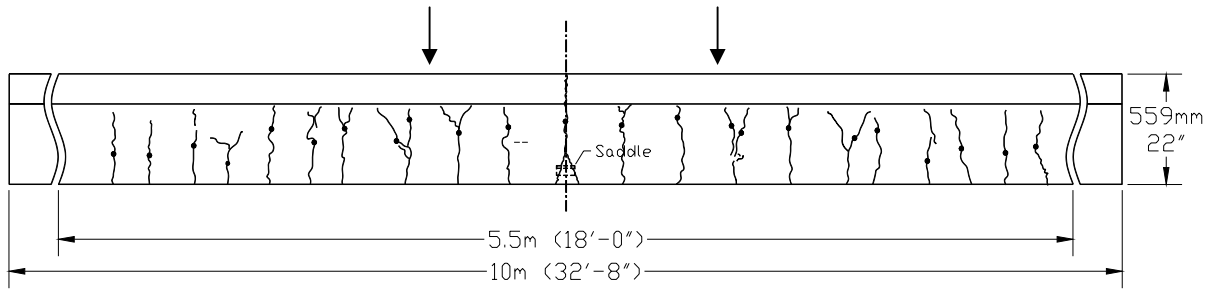
Figure 13.4 Carbon Crack Location
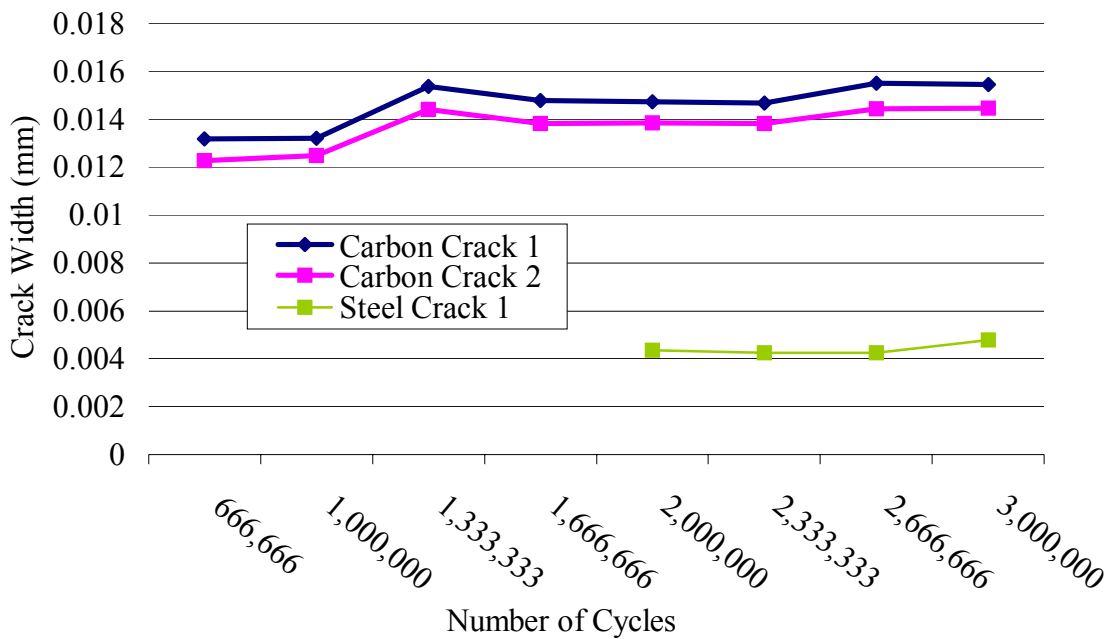
Figure 13.5 Crack Widths at Intermediate Static Tests

References

Abeles, P.W., et al., (1974) "Behavior of Under-Reinforced Prestressed Concrete Beams Subjected to Different Stress Ranges," Abeles Symposium on Fatigue of Concrete, SP-41, American Concrete Institute, Detroit, pp 279-299.

ACI 215 (1997),"Considerations for Design of Concrete Structures Subjected to Fatigue Loading", reported by ACI Committee 215, American Concrete Institute, Detroit.

PCI Design Handbook, 4th ed. (1992), Precast Concrete Institute, Chicago, pp. 4.36-38.

14.0 DUCTILITY OR DEFORMABILITY

Deformability is a key issue in determining the safety of FRP prestressed structures. Since FRP tendons do not exhibit ductility under the traditional definition, care must be taken to ensure that sufficient warning is exhibited prior to failure. Due to the lack of ductility, the concept of deformability and an index to measure performance provides a method of ensuring that this warning exists. Several approaches have been taken to quantify this concept into a deformability index, (Mufti 1996). This is usually accomplished through a ratio of deflections or curvatures under ultimate loads to those same quantities under service loads.

The use of an ultimate deflection to service deflection ratio gives an indication of the warning to failure, but there are two main problems with this approach. The first problem is that deflections for point loads or uniform loads on a simple span beam are simple to calculate, but deflections for continuous structures with various loads require rigorous analysis or the use of a computer analysis program. The deformability index is intended to be a design check and not a long and complicated design procedure. The second problem is the difficulty in determining the deflection under ultimate loads. Traditional approaches to calculating deflections for concrete members consider the softening effect due to cracking under service loads. Near ultimate loads, this softening occurs at a faster rate and is much harder to quantify.

Another approach is to use a ratio of the curvatures under ultimate and service loads. This is more easily accomplished by using quantities already calculated during the design process. The formula for this approach to the deformability index is as follows (Dolan 1996).

$$Index = \frac{(d - kd)\varepsilon_{FRP-Ultimate}}{(d - \dfrac{a}{\beta_1})\varepsilon_{FRP-Service}} \qquad (14\text{-}1)$$

Deformability indices were calculated for the harped prestressed beams tested and for beams from published data, Table 14.2. After examining the deformation indices, no trends were observed that could be directly correlated to "safe" behavior. If service loads are considered as the load to produce a tensile stress in the concrete of $3\sqrt{f_c'}$, the

decompression strains and the strain to produce $3\sqrt{f_c'}$ are very small compared to the prestress strain. The index is effectively a function of the ratio of ultimate strain to the prestressing strain with slight modification due to the differences in the neutral axis of elastic and inelastic behavior. Abdelrahman's indices are higher because the prestress was based on the manufacturers guaranteed strength (Abdelrahman 1997). Using Abdelrahman's reported ultimate strength from test on his CFRP, which was much higher than the manufacturer's, gives a higher index, but no further indication of safety or cracking. Abdelrahman intended to get 50 percent of ultimate, but with the higher actual stress they only achieved an initial prestress of 30 percent of f_{pu}.

Table 14.2. Indices and Ratios Used to Evaluate Deformability

	Condition	Deform-ability index	Ult./initial prestress	Max. defl./span	c/d ratio
Zhao[1]	Under-reinforced	2.3	2	1/36	0.269
Abdelrahman[2]	Under-reinforced	3.58	3.55	1/32	0.115
Abdelrahman[2]	Over-reinforced	4.4	3.55	1/32	0.345
Currier[3]	Over-reinforced	2.4	2	1/32	0.307
C1-H	Under-reinforced	1.79	1.67	1/67	0.0318

1. Zhao 1994
2. Abdelrahman 1997
3. Currier 1995

The data in Table 14.2 indicates that the most efficient method to obtain high deformability is to reduce the prestress. Reducing the prestress strain provides more tendon strain reserve, greater curvature or deflection capacity, and a higher index. The deformability index is nearly mimicked by the ratio of ultimate to initial prestress. A ratio of ultimate to initial prestress strain is easier to compute than the deformability index and provides similar results. A maximum prestress of $0.6f_{pu}$ assures a strain ratio of 1.67 or greater. The maximum deflection over span ratio for the beams is computed in Table 14.2. It can be seen that beam C1-H has less deformability that the other beams.

The specified deflection to span ratios vary from $^1/_{180}$ to $^1/_{360}$ for buildings and $^1/_{800}$ to $^1/_{1000}$ for bridges (ACI 318 1993, AASHTO 1994). The beams with deformability indices or strain ratios greater than two all had ultimate deformations eight to twenty times greater than specified deflection criteria. Beam C1-H had a final deflection only 6 times the ACI $^1/_{360}$ criteria and less than 3 compared to the $^1/_{180}$ criteria. This beam displayed a substantial deflection, over 5 inches, and substantial cracking prior to failure. However, the low reinforcement ratio and low difference between design and actual failure deflection suggests that this is close to the limit for deformability.

To expand on the behavior of beam C1-H, the ratio of c/d was examined, Table 14.2. A low c/d ratio implies a large strain demand on the tendon. Beam C1-H has a very low c/d ratio implying that the beam will have reached a high strain at a relatively low load. To preclude this behavior, a minimum amount of reinforcement is required. The requirements of AASHTO LRFD Bridge Design Specifications (1994) provide some guidance for establishing a lower bound c/d ratio.
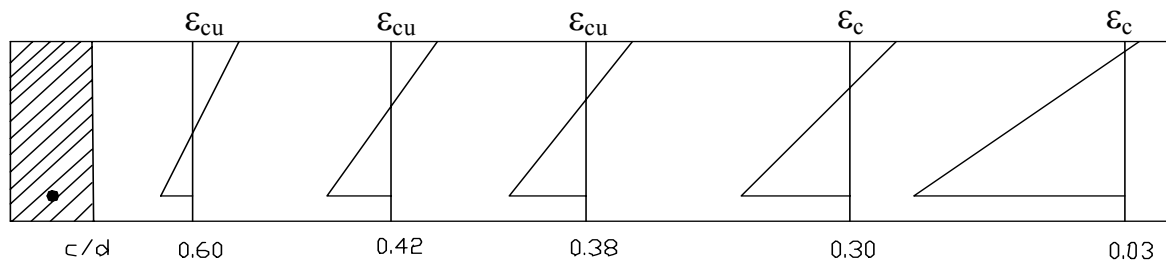
Figure 14.1. Strain gradient for various c/d ratios

The maximum reinforcement ratio is limited by c/d<0.42. Minimum limits required by AASHTO are that the amount of prestressed and non-prestressed reinforcement shall be adequate to develop a factored flexural resistance, M_r, at least 1.2 times the cracking strength. In addition, a limit is placed on the minimum reinforcement ratio, $\rho_{min} \geq 0.03\, f_c' / f_y$. If f_{pu} is substituted for f_y, this limit can be used to develop a limitation on the minimum c/d ratio for FRP prestressed beams as follows:

$$\rho_{min} = 0.03 \frac{f_c'}{f_{pu}} \tag{14-1}$$

and

$$a = \frac{A_s f_{pu}}{0.85 f_c' b} \tag{14-2}$$

Using the relationship $A_s = \rho b d$ and substituting this into equation 14-2 and substituting equation 14-1 into equation 14-2 the following is obtained

$$a = 0.035 d \tag{14-3}$$

Using the Whitney stress block relationship

$$c = \frac{a}{\beta_1} \tag{14-4}$$

gives the following limitation for a minimum reinforcement

$$\frac{c}{d} = \frac{0.035}{\beta_1} \tag{14-5}$$

The minimum c/d ratio in equation 14-5 will always be greater than the c/d ratio of beam C1-H. Since C1-H provided satisfactory performance, the deformability criteria for FRP prestressed beams may be satisfied by meeting the following criteria:

The ratio of ultimate tendon strain to initial prestress strain must be greater than 1.67. This is equivalent to a maximum initial prestress of $0.6 f_{pu}$.

Apply a prestress reinforcement ratio greater than $\rho_{min} = 0.03 \dfrac{f_c'}{f_{pu}}$.

14.1 References

AASHTO, *Standard Specifications for Highway Bridges*, *LRFD. US Customary Units,* Second Edition, American Association of State Highway and Transportation Officials, Washington, D. C. 1998.

Abdelrahman, A., and Rizkalla, S., (1997) "Serviceability of Concrete Beams Prestressed by Carbon Fiber-Reinforced Plastic Bars," ACI Structural Journal, American Concrete Institute, Farmington Hills, MI, Vol. 94, No. 4, July-August pgs. 447-457.

ACI Committee 318, (1999), "Building Code Requirements for Reinforced Concrete (ACI 318-99)," American Concrete Institute, Farmington Hills, MI.

Currier, J., (1995) "Deformation of Prestressed Concrete Beams with FRP Tendons," M.S., Department of Civil and Architectural Engineering, Laramie, WY.

Dolan, C. W. and Burke, C. R. (1996) "Flexural Strength and Design of FRP Prestressed Beams," Advanced Composite Materials in Bridges & Structures – 2nd

International Symposium, Canadian Society of Civil Engineers, Montreal, Quebec, Canada, pp. 383-390.

Mufti, Aftab A. and Newhook, John P., (1996). "Deformability Versus Ductility in Concrete Beams with FRP Reinforcement," <u>Advanced Composite Materials in Bridges and Structures</u>, M.M. El-Badry, editor, Canadian Society for Civil Engineering, Montreal, Quebec, pp. 189-199

Zhao, L., (1994) "Behavior of Carbon Fiber Composite Tendon Prestressed Concrete Planks Under Static and Fatigue Loading" M.S., Department of Civil and Architectural Engineering, Laramie, WY.

15.0 SHEAR

Material for this section is excerpted from Volume 2, Chapter 5.

This section examines beams with FRP shear reinforcement in addition to FRP longitudinal reinforcement. The basic finding of FRP stirrups is that the concrete contribution to shear resistance is reduced due to wider diagonal shear cracks. The total shear strength is further reduced because the FRP stirrups typically fail at the bend location. The following discussion examines the reduction of both the concrete contribution and the stirrup strength reduction to shear resistance.

From the assessment of the experimental to the theoretical nominal shear capacities, the following formulation for V_n is suggested for the modified ACI equations.

$$V_n = \beta\sqrt{f_c'}\,bd + \phi_{bend}\frac{A_v df_{pu}}{s}$$ (15-1)

where, $\qquad\qquad\qquad\qquad\qquad \beta \leq 2$

and $\qquad\qquad\qquad 0.25 \leq \phi_{bend} = \left(0.05\frac{r}{d_b} + 0.11\right) \leq 1.0$ (15-2)

In the above modifications of the ACI design equations, the V_c contribution has been limited to the minimum code restriction of $2\sqrt{f_c'}\,bd$. For the shear reinforcement contribution, the form remains unchanged except f_y is replaced by the stress of the FRP rod based upon its r/d_b ratio, as limited by equation 15-2. However, the formulation for ϕ_{bend} as suggested (Equation 15-2), is modified from the original JSCE formulation such that the minimum reduction factor is limited to 25 percent of the ultimate tensile stress of the FRP material. This was based upon the push apart tests performed on the aramid/nylon and carbon/nylon stirrups used, resulting in a ϕ_{bend} of 0.25. Hence, in the equation for the design stress of the FRP stirrups provided by the JSCE code, 0.3 has been reduced to 0.11. Moreover, the modified expression for ϕ_{bend} suggested, is more conservative than the form suggested by the JSCE code, consequently, Equation 15-2 is suitable for design applications until more refinement of the r/d_b response is available.

For the AASHTO formulations, the same ϕ_{bend} is suggested. However, no other modifications are made. In the concrete contribution, V_c of the AASHTO code, the

modified compression field theory predicts more conservative V_c values than the 45-degree truss model used in the ACI formulations. Consequently, the concrete contribution yields satisfactory results, and it is the V_s contribution that needs to be modified as shown in equation 15-3.

$$V_n = 0.0316\beta\sqrt{f_c'}\,b_v d_v + \phi_{bend}\frac{A_v f_{pu} d_v}{s}\cot\theta \qquad (15\text{-}3)$$

16.0 BOND, DEVELOPMENT AND TRANSFER LENGTH

Material for this section is excerpted from Volume 3, Sections A, F and I. .

FRP/concrete bond plays an essential role in the transfer of beneficial compressive load from one or more tendons to a structural element. Important issues to be resolved with FRP prestressing tendons include bond strength, bond durability, transfer length, and development length. Here, bond strength is defined load required for complete slip divided by nominal interfacial area between tendon and concrete. In prestressed concrete, transfer length is defined as the distance required to transmit the effective prestressing force from the prestressing tendon to the concrete. When a member is loaded to its ultimate flexural strength, an additional bond length beyond the transfer length is required to develop the tendon stress from the effective prestress to stress at failure of the member. This additional bond length is defined as flexural bond length, and the development length is defined as the sum of the transfer length and the flexural bond length.

In this investigation, bond was investigated by two methods: (a) the direct pullout test and (b) laboratory-scale prestressed beam tests. The direct pullout test is a widely used, compact, and economical test that provides a relative measure of bond strength among tendons tested under comparable conditions such as embedment length and environmental exposure. The tendons are cast inside of blocks of concrete having enough cover so that the blocks do not split during slip. The bonded portion of the embedment length is restricted to a central volume of the block to avoid end effects. Laboratory-scale beam tests enable the evaluation of methods for prestressing beams and important design parameters that cannot be measured in direct pull-out tests – namely, transfer length, development length, and nominal bond strength over the development length. The types of FRP tendons included in the experiments are the commercial Leadline (CL) and Technora (AT) products as well as the generic Strawman (CS) tendon developed for this research preject. The following discussion briefly reviews the methods and findings of the two investigations pertaining to bond.

16.1 Bond of Conditioned and As-Received Tendons by the Direct Pull-Out Test

Procedures

Half of the tendons were conditioned for 28 days in a high alkaline solution of $Ca(OH)_2$ and water held at 80°C to accelerate the service environment in moist concrete. The pH level of the saturated solution was between 12 and 13. After conditioning, the tendons were removed and allowed to dry in an indoor laboratory environment for 14 days before casting into concrete pullout specimens. Bond length, l_b, was selected on multiples of the nominal diameter of each tendon type ($2.5d_b$, $5\ d_b$, $10\ d_b$, and $15\ d_b$). Three or four replicates were done in each type of test and the mean was computed. The concrete block was 152-mm cube with the tendon penetrating through the center. The size and strength of the concrete block were designed to prevent splitting of the block, based on prior experience by the investigators. Three or four replicates were done in each case and the mean and standard deviation were computed. No attempt was made to determine the level of confidence in these statistical parameters.

During pullout testing, slip was measured with LVDTs situated at the loaded and free ends of the embedment length. Load was quasi-statically increased until several mm slip at the fee end had occurred. Bond strength – maximum load divided by nominal bond area – was calculated as follows:

$$\tau = P/(\pi d_a b_{ble}) \qquad\qquad (16\text{-}1)$$

where P is the maximum load on the load-slip curve. The results are summarized in the bar chart in Figure 16.1.
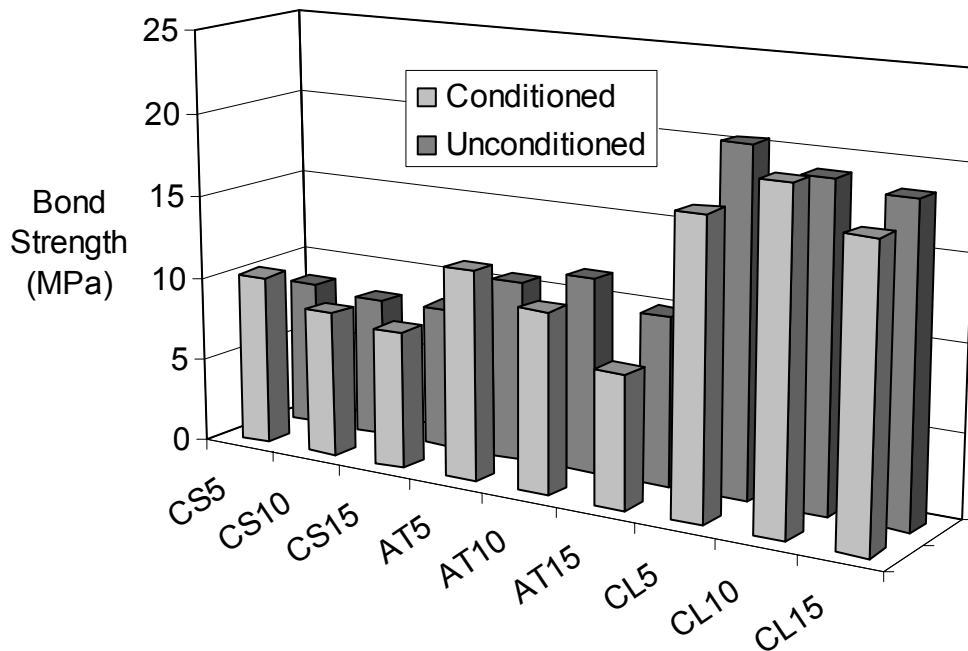
Figure 16.1 Bond strengths of conditioned and unconditioned FRP tendons in direct-pull-out tests.

Results

On the whole, the FRP tendons used in this investigation were not significantly affected by this conditioning regimen. Averaged over all bond lengths, the average change in bond strength due to conditioning was less than ±10 percent, which is not considered significant in light of comparable coefficients of variation for bond strength among replicate tests. It is therefore concluded that all three FRP tendons are rather resistant to the highly alkaline aqueous $Ca(OH)_2$ environment.

A very slight decrease in bond strength with longer bond lengths was observed in this investigation. In all experiments where only bond failures occurred, slip of FRP tendons was governed by shear failure of the material on the surface of the tendon rather than by failure of the concrete. A few of the specimens failed by either grip-induced stress concentration or by splitting of the concrete prior to attainment of ultimate bond strength. Concrete blocks having a cover of approximately 6-9 bar diameters provided adequate confinement in most of the cases, but it appears that more confinement may be

needed in situations with greater than $10d_b$ bond length. Experiments that ended in concrete splitting were omitted from the comparisons of bond durability made here.

While it is not clear at this time how much bond strength is optimal, it can nonetheless be concluded that Leadline tendons had the highest bond strength of all tendons and tendons used in this investigation. These tendons apparently have an advantageous combination of transverse stiffness and mechanical interlock. In the unconditioned tests, Leadline had bond strengths greater than or equal to that of epoxy-coated steel bars (19-21 MPa). The relatively low bond strength of the Strawman tendon is attributed to the relatively small surface indentation since the transverse stiffness of this tendon should be similar to that of Leadline. The Technora aramid tendon had larger lugs than either carbon tendon, but this potential for greater interlock did not translate to improved bond strength versus Leadline. Hence, it is clear that surface geometry alone does not dictate the bond behavior of FRP tendons. Additional factors, such as material properties and construction methods, also affect bond performance.

The overall ranking of the three tendons, in terms of bond strength, is Leadline, followed by the closely ranked Technora and Strawman. In the following section, it is shown that a similar trend is observed when the average bond stress is calculated from prestressed beam development length test results. It is therefore apparent that the direct-pullout test provides a reasonable relative measure of bond performance of FRP tendons that is simple and economical and amenable to accelerated environmental testing.

16.2 Transfer Length, Development Length, and Bond in Prestressed Lab-Scale Beams

16.2.1 Procedures

The Leadline (CL), Technora (AT), and Strawman (CS) tendons were used to fabricate prestressed laboratory-scale beams. For comparison, conventional 7-wire uncoated steel strand was also used. In each case, the nominal diameter of the tendon was 8 mm. The aim of this portion of this task is to evaluate a method of prestressing beams with FRP tendons and to evaluate critical design parameters such as transfer

length, development length, and nominal bond strength over the development length. One tendon was placed either on center or eccentrically in the cross-section. No other reinforcement was used in the beams. The beams were designed for balanced failure in the cases of Leadline and steel.

To assure a minimum loss of strength in the FRP tendons due to anchorage, the tendons were fitted with steel anchors filled with expansive cementitious grout as described in Appendix I. These anchors have proven to be highly effective in terms of strength and long-term durability in the laboratory. The anchors were applied in the laboratory, prior to shipment of the FRP tendons to the commercial prestressing plant. The anchors were placed at opposite ends of the coiled tendon and had threaded outside diameters that were later interfaced with internally threaded steel pipes that served as reusable couplers. The couplers joined the FRP tendon with short (1.5-m) steel tendons similarly equipped with one steel grouted anchor. The outboard ends of the steel tendons were fitted with no anchors so that they could be gripped with conventional steel prestressing anchors on a conventional 18.3-m-long prestressing bed. A total bed length of only 3 m or so was lost with this arrangement, and time-consuming casting of cementitious anchors at the plant was completely avoided.

Due to the brittle nature of FRP materials, it is recommended that 8-mm-dia. tendon be coiled for shipment into a circle no smaller than 2.1-m-dia. A coil of this diameter results in a maximum strain of ±0.4 percent in the tendons, which is no greater than 1/3rd the short-term failure strain of the most brittle system included in the research. No signs of distress have been seen in any of the three tendons that have been continuously coiled in this manner for three years. However, the Technora aramid tendon tends to develop a small degree of curvature set that is easily eliminated with a small tensile load on the uncoiled material and does not seem debilitating in terms of performance.

Jacking stresses of 60-65 percent of ultimate were used for the lab-scale beams. After the steel anchors were set at the plant and the tendons were allowed to relax for two hours prior to pouring concrete, prestress losses were noted to be between 9 and 14 percent in all cases, including steel. The Technora and Strawman tendons were at the

high end of this spectrum and Leadline and steel were at the low end. Leadline had the least initial loss.

Transfer length was measured using a Whittemore type extensometer and detachable targets bonded onto the beam at the level of the tendon. Measurements were made at 50 percent and 100 percent of release and at 28 and 90 days. The average values of measured concrete strain were plotted versus distance along the length of each specimen to generate a strain profile for each specimen at each time interval. Transfer lengths for each specimen were determined by evaluating the concrete strain profiles. The method used in this study is as follows:

1. Plot the smoothed strain profile versus longitudinal position in the beam.

2. Determine the average maximum strain for the specimen by computing the numerical average of all the strains contained within the strain plateau. The plateau is determined by visual inspection. Calculate 95 percent of the average maximum strain and construct a horizontal line through the data corresponding to this value.

3. Transfer length at each end of the beam is determined by the intersection of the 95 percent line with the smoothed strain profile. Reported values of transfer length are the average values from the two ends of the beam. The average maximum strain is computed by averaging all the strains contained on the plateau of the fully effective prestressing force.

Development length was measured by applying an eccentric third-point load at progressively larger lever arms relative to one end of the beam until a flexural failure rather than a bond-slip failure resulted. The shortest lever arm that causes a flexural failure (in these cases, compression/shear failure) is defined as the development length. A maximum development length, defined as the bonded length needed to develop the nominal design strength of the tendon, was also evaluated with the assistance of a flexure model that enabled the calculation of tendon force in each test. With the tendon force associated with tendon slip known for each test, an extrapolation of lever arms to the value needed for the tendon to reach the design strength could be made, even though the

design strength was not actually ever reached in the experiments. Furthermore, the average bond stress over the length of tendon corresponding to the development length can also be calculated by this method. Details of the procedure are given by Lu (1998).

A number of equations for predicting the transfer and development lengths were taken from the literature and applied to the experimental conditions at hand. The ACI 318-99 equations (ACI 1999) for transfer and development lengths (in inches) of steel twisted strand are repeated here as eqs. 16-2 and 16-3, respectively, for use with US customary units:

$$L_t = \frac{1}{3} f_{se} d_b \qquad\qquad (16\text{-}2)$$

$$L_d = \frac{1}{3} f_{se} d_b + (f_{ps} - f_{se}) d_b \qquad\qquad (16\text{-}3)$$

where f_{se} is the effective prestress after all losses (ksi), f_{ps} is the stress in the tendon at flexural failure of the member (ksi), and d_b is the nominal diameter of the tendon (in.).

Results

The results of the transfer length and development length experiments are shown in the histogram in Fig. 16-2. Comparisons with the ACI equations are given in Table 16-1. The following conclusions are made:

1. The transfer length results for the Leadline and Technora tendons in this study were verified to be close to values reported by other investigators using similar materials and measurement methods.

2. Despite differences in tendon material properties and prestressing forces, the measured transfer lengths were virtually identical for all three FRP materials. The steel strand had a slightly longer transfer length than the FRP tendons.

3. The transfer length predicted by the ACI formula is in direct proportion to the effective prestress f_{se} in the tendon. However, the results of this study indicate that the transfer length for FRP tendons is very little influenced by prestressing level. Since the f_{se} was lower for AT and CS in this study, the transfer lengths of

these two materials were poorly predicted by the ACI equation. Use of a formula that is solely based on tendon diameter may give better predictions, especially for materials with lower initial prestressing levels. The adoption of a minimum value of transfer length, as in the AASHTO Design Specification, improves this result, although 50 tendon diameters, as in previous editions of the code, may be a better estimate for FRP than the 60 diameters prescribed in the present edition (AASHTO 1998).

4. Despite differences in tendon material properties and prestressing forces, the maximum measured development lengths were almost equal for all three FRP materials and the steel strand tested in this study.

5. The FRP materials consistently had a nominal bond stress (pull-out force divided by nominal surface area at the development length) significantly greater than the 1.98 MPa value of steel tendons. The bond stresses in Leadline, Technora, and Strawman were 3.68, 3.13, and 3.21 MPa, respectively. Aside from a switch of the closely ranked Technora and Strawman tendons, this trend is similar to that observed in the direct-pullout tests discussed earlier in this report.

6. The development lengths of the three FRP tendons were could be conservatively predicted by a modified ACI design equation that uses strand rupture strength in place of f_{ps}, strand stress at nominal strength of the member.

7. A number of other models, including models developed specifically for FRP tendons, give wide-ranging development length results, most of which are over-estimations compared to the ACI equation. While it may seem obvious that formulas developed for steel tendons do not give good predictions for FRP tendons, it is worth considering the reasons for this, namely that the higher bond stress of the FRP tendons results in shorter development lengths.

8. It is recommended that a transfer length of at least 50 tendon diameters be used for FRP tendons.

9. The interest in calculating the development length conservatively may account for the large overestimate produced by many of the existing models, for steel as well

as FRP strands, but the existing code philosophy appears to suggest that an average value of the transfer and development length should be calculated.

10.   It is recommended that the rupture strength of FRP tendons, f_r, be used, rather than the stress at the nominal flexural strength of the cross-section f_{ps}, in calculating the flexural bond length of FRP tendons. It is further recommended that the development length formula take into account the higher bond stress developed by FRP tendons, so that development length is not calculated excessively conservatively. Because most prestressed concrete beams are under reinforced, use of f_r is consistent with actual behavior.

A proposed equation addressing both points of the last conclusion is as follows:

$$L_d = \frac{1}{3} f_{se} d_b + \frac{3}{4} (f_r - f_{se}) d_b \qquad (16\text{-}4)$$

Dividing the predictions by this equation to the measured values of development length results in values of 1.63, 1.46, 1.38, and 0.95 for Leadline, Technora, Strawman, and steel, respectively. When dividing the same predictions by the calculated maximum development lengths (i.e., those needed to fail the tendons), the values are 1.59, 1.24, 1.35, and 1.05 for the same series of tendons. This equation is therefore conservative not only for the FRP results generated in the current investigation, but also those generated elsewhere.

The experience of fabricating the specimens has indicated that the anchorage of the prestressing tendon is a key issue to be resolved before widespread implementation of FRP prestressing is possible. Whereas an anchor based on the use of expansive grout will develop the strength of the tendon effectively, the long time period required for the grout to cure results in inefficient use of the prestressing beds. The coupling anchors used in this study would allow the precasting beds to be turned over quickly, and less than 2-3 percent of the bed would be lost due to the coupling.
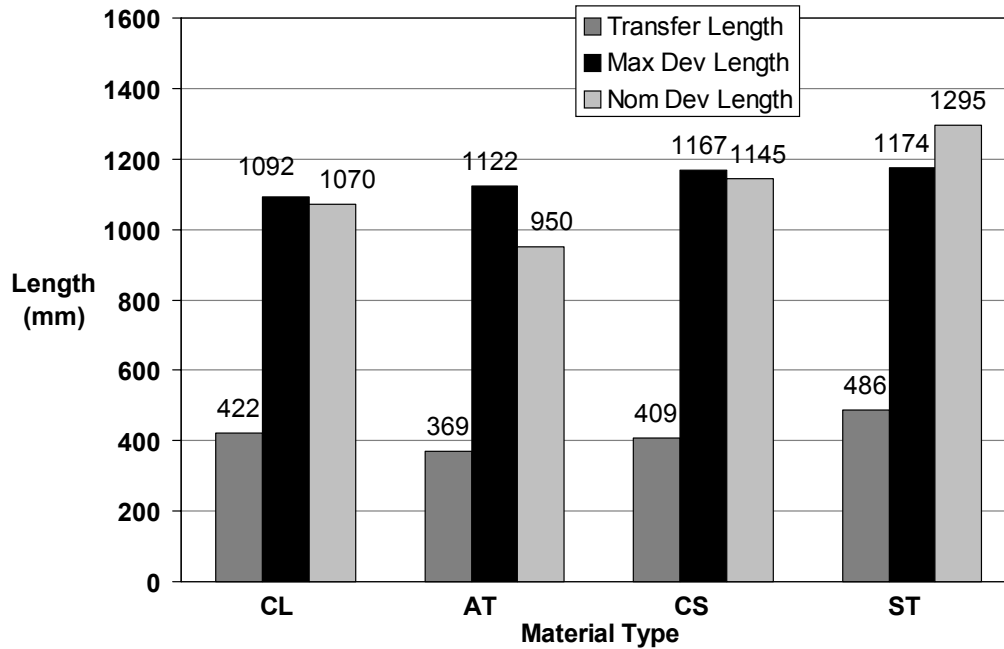
Figure 16.2. Summary of results for lab-scale beams: transfer length, maximum development length, and development length.

Table 16.1. Measured transfer and development lengths (L_t and L_d) in comparison with the ACI-318 equations for steel tendons.

Tendon	L_t (ACI) mm	L_t (100%) mm	$\dfrac{L_t \text{ (ACI)}}{L_T}$ (100%)	L_d (ACI) mm	L_d (Exp.) mm	$\dfrac{L_d \text{ (ACI)}}{L_d \text{ (Exp.)}}$
CL	416	422	0.98	1740	1070	1.62
AT	300	369	0.81	904	950	0.95
CS	328	409	0.80	1578	1145	1.38
ST	380	486	0.78	1232	1295	0.95

16.3 References

AASHTO, (1998) *Standard Specifications for Highway Bridges, LRFD. US Customary Units,* Second Edition, American Association of State Highway and Transportation Officials, Washington, D. C.

ACI Committee 318, (1999) "Building Code Requirements for Reinforced Concrete (ACI 318-99)," American Concrete Institute, Farmington Hills, MI.

Lu, Z., (1998) "Flexural Performance of Fiber Reinforced Polymer Prestressing Tendons," M.S. Thesis, The Pennsylvania State University, University Park, PA

16.4 Notation

d_p	=	depth of prestressing reinforcement
E_c	=	elastic modules of the concrete
I_{cr}	=	cracked moment of inertia
I_e	=	effective moment of inertia
I_g	=	gross moment of inertia
I_{rep}	=	moment of inertia for repeated loading
k_p	=	factor for the calculation of the deflection due to the prestressing reinforcement, depends on the shape of the strand
k_s	=	factor for the calculation of the deflection due to the applied loads depends on the shape of the loading and boundary conditions
M_{cr}	=	cracking moment
M_{dc}	=	decompression moment
M_{rep}	=	moment due to repeated load
M_s	=	service moment
L	=	span of the beam
P_{dc}	=	decompression load
P_e	=	effective prestressing force
P_{rep}	=	maximum repeated load
y_{cr}	=	distance between the centroid of the section and the compression fibre based on cracked section properties
y_e	=	distance between the centroid of the section and the compression fiber accounting for tension stiffening, calculated at one section or along the beam
y_g	=	distance between the centroid of the section and the compression fiber based on gross section properties
Δ	=	deflection of the beam
Δ_r	=	residual deflection of the beam after removal of the load

APPENDIX I

Test specification For Test Methods to establish tensile properties of continuous Fiber Reinforced Polymer tendons

Specification for Test Methods to Establish Tensile Properties of Continuous FRP Tendons

SPECIFICATION	*COMMENTARY*

1. SCOPE

A procedure is presented for the determination of short-term tensile properties of FRP tendons for prestressed concrete structures. The output of the performance characterization of FRP tendons.

2. REFERENCED DOCUMENTS

ASTM Documents

- *D 792*-Test Methods for Specific Gravity (Relative Density) and Density of Plastics by Displacement

- *D 883*-Terminology Relating to Plastics

- *D 2584*-Test Method for Ignition Loss of Cured Reinforced Resins

- *D 2734*-Test Methods for Void Content of Reinforced Plastics

- *D 3171*-Test Method for Fiber Content of Resin-Matrix Composites by Matrix Digestion

- *D 3916* - Test Method for Tensile Properties of Pultruded Glass Fiber-Reinforced Plastic Rod

- *D 5229* - Test Method for Moisture Absorption Properties and Equilibrium Conditioning of Polymer Matrix Composite Materials

- *E 4*-Practices for Force Verification of Testing Machines

- *E 6*-Terminology Relating to Methods of Mechanical Testing

- *E 83*-Practice for Verification and Classification of Extensometers

- *E 177*-Practice for Use of the Terms Precision and Bias in ASTM Test Methods

- *E 456*-Terminology Relating to Quality and Statistics

- *E 1237*-Guide for Installing Bonded Resistance Strain Gages

ASTM documents that examine the various aspects of the testing procedure are referenced.

3. TERMINOLOGY

- Terminology D 3878 defines terms relating to high-modulus fibers and their composites.

- Terminology D 883 defines terms relating to plastics.

- Terminology E 6 defines terms relating to mechanical testing.

- Terminology E 456 and Practice E 177 define terms relating to statistics. In the event of a conflict between terms.

- Terminology D 3878 shall have precedence over the other standards.

4. SUMMARY OF TEST METHODS

A FRP tendon is mounted in the grips of a mechanical testing machine and monotonically loaded in tension to failure while recording the load and strain.

5. SIGNIFICANCE AND USE

From a tension test a variety of data are acquired that are needed for design purposes. The properties that can be obtained during this type of testing are the ultimate tensile strength and strain, the tensile modulus of elasticity, and physical characterization.

6. TEST INTERFERENCES

- The results from the procedures presented are limited to the environment in which it is tested. If the tendons are to be used in extreme environmental conditions then the test should attempt to model the conditions.

- Gripping of the tendons has been known to cause premature failures in specimens. Anchors should be designed in such a way that the full tensile capacity can be achieved during the test.

- Due to fabrication of the materials, there tends to be variable strength parameters even within those produced form the same manufacturer.

- Improper alignment of the tendon within anchors or the testing machine can produce lower results due to bending of the material.

Care shall be taken to insure that the test will provide only axial forces to the specimens, in the intended environment of use, and that proper modes of failure will be achieved. Refer to Section 8 for additional guidance.

SPECIFICATION	_COMMENTARY_

7. TESTING APPARATUS

7.1 _Tendon_

- Any method for cutting test samples shall be permitted as long as the process does not impair any of the fibers in between the anchors.

- The diameter and length of the test sample shall be recorded using a micrometer with a resolution no greater than 0.025 (0.001 in) and a standard tape measure with a resolution of no greater than 1 mm (.04 in). For non-uniform sections, the nominal diameter shall be recorded.

7.2 _Testing Machine_

- The testing machine shall be calibrated in conformance with Practice E 4.

- The machine shall have a loading capacity in excess of the tensile capacity of the test piece.

- The machine shall have both an essentially stationary head and a movable head.

- The machine should be driven is such a way as to specify the moveable head velocity with respect to the stationary head.

- A load indicator, free from inertia-lag, must measure the load within an accuracy of $\pm$ 1% of the indicated value.

- The machine must be capable of gripping the specimens in such a manner that the load is applied in coincident with the longitudinal axis of the specimen and also prevents slippage between the grip face and the specimen.

7.3 _Strain Indicating Device_

- The strain shall be recorded by either a strain transducer or an extensometer as long as attachment of these devices does not cause damage to the specimen surface.

- Strain gages shall have an active gage length of 6 mm (0.25 in) for most materials with a minimum length not less than 3 mm (0.125 in). The method of attachment should consider the type of material that is being tested.

- ASTM E1237 describes the procedure for surface preparation of specimens for application of strain gages, however the gage manufacturer should be consulted for specific instructions on application of the gage to the specific surface.

- The gage or extensometer should provide an accuracy of 10×10^{-6}

- Extensometers shall satisfy, at a minimum, Practice E 83.

- The distance from the points where the device is fastened should

For most tendons the application of strain gages is impractical due to surface conditions of the specimens (i.e. braided, twisted, and other deformations). It is therefore suggested that extensometers be used when testing FRP tendons.

The extensometer shown in Exhibit 1 has been demonstrated to be suitable for FRP tendon testing. It is not usually damaged when the tendon fails.

be at least 8 diameters from the anchors and centered on midspan of the specimen.

- For determination of the modulus of elasticity, two extensometers shall be placed back-to-back on the specimen at the midspan to determine if bending is occurring in the specimen.

8. TEST SPECIMENS

8.1 *Length*

- The specimen shall be cut to a length so that there is sufficient length for anchorage and a minimum of 40 bar diameters between anchors and not greater than 70 diameters, but not less than 100 mm (4 in)

- The length of the tendon between the anchors shall be recorded to the nearest 6.0 mm (0.25 in).

Tests have shown that there is no significant statistical influence of varying the length of the tensile specimen between 40 and 70 diameters.

Japanese recommendations specify that the length of the test specimen shall be greater than 100 mm (4 in) and greater than 40 bar diameters.

8.2 *Tendon Dimensions*

- The diameter shall be recorded at three points along the test length with the average value noted in conjunction with ASTM D 3916.

- In cases where the surface of the sample is severely ribbed making it impossible to record accurate diameters, the pycnometer test may be run to determine the tendon dimensions.

- In all cases, the nominal diameter shall be reported.

Research has shown that pycnometer samples should be at least 200 mm (8 in) long to provide accurate results.

Manufacturers report the dimensions of their specimens in accordance with the nominal values, however, for testing specimens it is essential that the actual values be considered.

8.3 *Number of Specimens*

- A minimum of 6 specimens shall be tested.

- If the test specimen is found to have clearly failed at the anchorage section, or found to have slipped out of the anchor, the results shall be discarded and the number of anchor failures shall be reported. Additional tests shall be performed.

SPECIFICATION	*COMMENTARY*

8.4 *Anchorage*

- Anchorage of the specimens will not be required if the testing machine is able to grip the specimens without causing damage.

- The type of anchors used is limited only to being capable of transmitting loads to the tendon in such a manner that failure will occur in the test section and not at the anchorages.

  .

Many anchoring systems have proven effective in the various completed research projects around the world. The system employed should be proven to its effectiveness to insure full capacity can be reached.

Expansive cement anchors have been demonstrated to satisfy these requirements and are described in Exhibit 2.

Failure of high volume fraction tendons makes determination of the original failure location difficult.

8.5 *Material Properties*

- Tendon manufacture shall supply constituent material quantities, i.e. volume fraction.

- If required, properties shall be verified using test methods described in the commentary.

Specific gravity and density may be verified by means of Test Methods D 792.

Volume percent of the constituents may be evaluated by one of the matrix digestion procedures of Test Method D 3171, or for certain reinforcement materials such as glass, by the matrix burn-off technique of Test Method D 2584.

The void content equations of Test Methods D 2734 are applicable to both Test Method D 2584 and the matrix digestion procedures.

9. CALIBRATION

The accuracy of all testing equipment should have certified calibrations at the time of testing.

SPECIFICATION	COMMENTARY

SPECIFICATION

10. CONDITIONING

- Specimens to be tested shall be placed in the testing environment one week prior to testing.

11. PROCEDURE

- Testing equipment should be validated for calibration as discussed in Section 9.

- Specimens shall be prepared as discussed in Section 8.

- The material should be conditioned as discussed in Section 10.

- Place the specimen in the grips of the testing machine, taking care to align the long axis of the gripped specimen with the test direction. Tighten the grips, recording the pressure used on pressure controllable (hydraulic or pneumatic) grips.

- If strain response is to be determined attach the strain-indication transducer(s) to the specimen, symmetrically about the mid-span, mid-width location. Attach the strain recording instrumentation to the transducers on the specimen.

- Set the speed of testing to obtain a nearly constant rate in the gage section. The elapsed time of the test from the initial application of load until failure shall be not less than two minutes nor more than 8 minutes. The constant rate may be defined in terms of the following:

>   Constant loading rate.
>
>   Constant strain rate.
>
>   Constant Head Speed Tests.
>
>   Elapsed time.
>
>   Constant Vernier setting

COMMENTARY

ASTM D5229/D5229M reports on a specific environment in which to condition specimens. However, research has shown there is no need for special conditioning of FRP materials prior to testing. This is consistent with the Japanese research, which does not mention a need for a conditioning procedure as long as the tendon properties are not impaired by the environment where they are placed.

Parametric studies of FRP tendon loading rates confirm that the 2-8 minute time duration avoids both impact loading and creep-rupture effects.

For automatic test machines, constant load, strain, or head speed (stroke) may be established by dividing the failure capacity by the mean time duration.

For manual test machines, the vernier setting shall be established to require no adjustments from the time of initial load application until failure.

SPECIFICATION	_COMMENTARY_

- Apply the load to the specimen until failure occurs while recording load and transducer strain or displacement data.

- Record load versus strain, or transducer displacement, continuously, or at frequent regular intervals. If the specimen is to be failed, record the maximum load, the failure load, and the strain, or transducer displacement, or as near as possible to, the moment of rupture.

Exhibit 3 contains a sample data sheet.

- Record the failure mode

12. CALCULATION

- Reduce displacement data to strain.

- Compute the mean break load and standard deviation.

- Compute the mean strain and standard deviation.

- Provide plots of load versus strain.

- Compute the modulus of elasticity based on the nominal area over 50 points in the linear portion of the curve.

The precedence for plotting load versus strain is that this eliminates the need for artificial stress calculations resulting from various cross sectional area properties, which may be difficult to obtain.

13. REPORT

Reports for the testing should include the following information or references pointing to other documentation containing this information.

Exhibit 3 is a sample test report form.

13.1 _General Information_

- Names of the test operator(s)

- Date, time, and location of the test

- Test number of the series out of the total number tested

- Data file to which the information is associated

- ASTM documents that are being referenced

13.2 _Material Data_

- Material type and manufacturer, type, and any other data used to specifically describe the material

- Method of specimen preparation including labeling scheme, sampling method, and cutting method

- Report the density, volume fraction, and void content and the procedures used to evaluate these properties. Properties may be provided by the manufacturer

- Results of any non-destructive tests

- Dimensions of each specimen

- Surface geometry

- Conditioning procedure

13.3 _Testing Equipment_

- Testing machine used along with calibration date and method

- Transducer types, range, and placement along with calibration information

- Data acquisition equipment and sampling rate

13.4 _Testing Parameters_

- Temperature and relative humidity of laboratory, or the environment of the testing machine environmental chamber (if used)

- Procedure to control rate of loading

- Problems occurring during the test

- Noted variations from this procedure

13.5 _Results_

- Plot showing the load versus strain of the material and the corresponding data

- Mean ultimate strength and strains

- Mean Modulus of elasticity

- Failure mode and location

- Average value, standard deviation, and coefficient of variation for the entire population

- Design break strength equal to the mean strength less 1.65 standard deviations

- Classification of the tendon

Exhibit 4 contains a test summary form

Specification for Test Methods to Establish

Tensile Properties of Continuous FRP Tendons

Exhibit 1 – Low cost FRP Tendon Extensometer
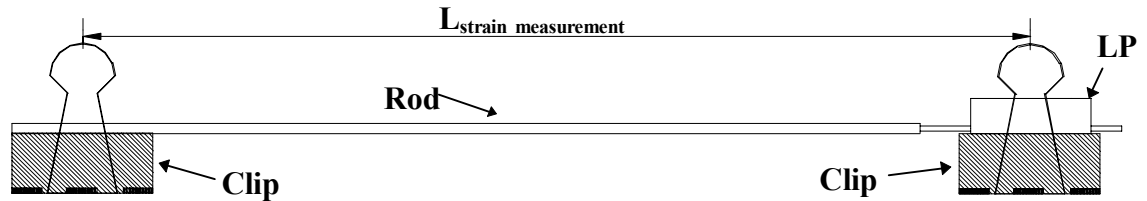
The strain is measured using a linear potentiometer (LP). The LP is placed on the end of a rod to allow strain measurements over a longer gage length. The LP is attached to the tendon using a clipping device adhered to the ends of the rod and the LP. The clamps were then attached to the specimen at points away from the anchorage as required in the testing procedure. A flexible plastic sleeve was placed over the tendon in the areas where the clamp was placed to avoid damage to the surface. For each specimen two of the LP setups were placed back to back and the average strain of the two was recorded.

Specification for Test Methods to Establish

Tensile Properties of Continuous FRP Tendons

<u>Exhibit 2 - Bristar Expansive Cement Anchors</u>

Materials

- Bristar Expansive Cement
- Water
- Mixer
- Scale
- Graduated Cylinder

- Mixing Container
- ≥12" long ¾" diameter Steel Pipe
- 2-Stoppers per anchor
- Drill w/ bits
- FRP Tendon

Procedure

1. Take the stoppers (#3 stoppers for ¾" diameter steel pipes) and drill a center whole to the tendon size. The procedure is made easier if stoppers are purchased with pre-drilled holes thus the holes only need to be widened. Normal drill bits may be used and the stopper can be held by grips or hand held.

2. Cut the FRP tendon to length.

3. Devise a frame allowing the steel pipes to be placed vertically.

4. For the top anchor, slide a drilled stopper down over the tendon (roughly 1"+ anchor length from the top) and place the steel pipe down on the stopper in such a fashion that fluid may not leak out the bottom. The second stopper will be used to center the tendon at the top of the anchor after pouring the cement. See figure below.

5. For the bottom anchor slide a stopper up from the bottom of the tendon (roughly 5" + anchor length from the bottom). Slide the steel pipe up and place the other stopper at the bottom of the tendon. The pipe then is slid down and secured so no leaks will occur. The first stopper applied will be slid down to center the tendon in the anchor. See figure below.

**Top
Anchor**

**Bottom
Anchor**

6. Mix a batch of Bristar expansive cement. Using the scale measure out a specified amount of Bristar. Fill the graduated cylinder with the specified amount of water. For 2 ¾" steel pipes 12" long the specified amounts were 0.75 lbs of Bristar and 100 mL of water. This ratio was successfully scaled for multiple anchors and for anchors of different length and diameter. Pour the specified amounts into a mixing container and stir the cement for one minute with a mixer.

7. Once the Bristar is thoroughly mixed, pour it into the steel pipes that is set up in the vertical configuration devised in step 3.

8. Once the Bristar is in the pipes, apply a stopper to the top of the pipe and carefully slide down to center the tendon in the top. Be sure to hold the bottom stopper and pipe while sliding the stopper down so the bottom stopper won't lose its seal. Finally slide the top stopper on the bottom anchor down to center the tendon in the bottom anchor.

9. Let the cement cure for 48 hours (preferably in a moist environment) before use.

Final Anchorage Setup

Specification for Test Methods to Establish

Tensile Properties of Continuous FRP Tendons

<u>Exhibit 3 - FRP Tendon Tensile Test Report</u>

Material_____ Test Operator _____

Test #_____ Location _____

Data File _____ Date_____

ASTM Document_____ Time_____

<u>Material Data</u>

Manufacturer_____ Length _____

Material Type _____ Diameter_____

Density _____ Area _____

Volume Fraction_____ Surface Geometry_____

Specimen Preparation_____

_____

Anchorage System_____

Curing Procedure_____

_____

<u>Testing Procedures</u>

Testing machine_____

Data Acquisition_____

Calibration dates and methods_____

Strain Device Information _____

Strain Device Range and Placement_____

Hydraulic Grip Pressure_____

<u>Test</u>

Relative Humidity_____

Temperature_____

Environment of chamber (if used) _____

Procedure to control loading rate _____

Problems occurring during testing _____

_____

Noted Variations From ASTM Procedure_____

_____

_____

Appendix II – Recommended Changes to aashto SPECIFICATION

Introduction

The following recommendations are arranged by the section numbers of the AASHTO LRFD Bridge Design Specifications, SI Version, First Edition, 1994. Suggestions for incorporation of FRP tendons are placed in either the Specification or Commentary portion depending on which is most appropriate. The recommendations are based on the material presented in this final report. Where appropriate, section numbers from the Final Report are provided to assist in evaluating the intent of the recommendation.

Recommended Changes to AASHTO Specifications

5.2 Definitions

add

FRP – fiber reinforced polymer

CFRP – carbon fiber reinforced polymer

AFRP – aramid reinforced polymer

GFRP – glass reinforced polymer

A_f – Area of FRP tendon

f_{fu} – Tensile capacity of FRP tendon, MPa

E_f – Modulus of Elasticity of FRP Tendon, GPa

5.4.4.2 Modulus of Elasticity

C5.4.4.2

The modulus of elasticity is dependent on the fiber and the fiber content of the FRP tendon. It should be obtained by test or from the manufacturer.

Prestressing Steel - General

C5.4.4.1

The manufacturer shall supply the properties of FRP tendons.

Appendix I contains a test methodology that provides strength, strain and modulus data for FRP tendons.

5.4.6.3 Ducts at a Deviation Saddles

Deviation saddles for FRP tendons should have a radius of not less than 0.9 m (30 in.) In addition, the saddle must be designed so the tendon does not cross a sharp edge on the saddle

5.5.3.3 Fatigue

Conventional Construction

The Resistance factor ϕ shall be taken as:

• Flexure and tension of prestressed concrete

CFRP tendons	0.85
AFRP tendons	0.70

Shear and torsion

normal weight concrete   0.85

5.5.4.4.2 Segmental Construction

5.7.3.1.1 Component with Bonded Tendons

C5.4.6.3

The tendon stresses at deviators must be included in the tendon stress analysis. (Section 7.2).

C5.5.3.3

CFRP prestressing tendons have fatigue properties superior to steel tendons. (stress range values for steel tendons may be used for FRP tendons. (Section 13)).

C5.5.4.2.1

(Section 8.6)

v_c must be limited to $2\sqrt{(f'c)}$ and the strength of the stirrup must be reduced by ϕ_{bend}

Section 15 describes ϕ_{bend} and must be added to the Specification.

C5.5.4.4.2

No data for the use of FRP tendons in segmental construction exists at this time. Consequently, this report makes no recommendation on the use or non-use of FRP tendons for segmental construction.

C5.7.3.1.1

For bonded prestressed beams the tensile capacity of the tendon is identical to the tensile strength of the tendon and thus iterative or empirical solutions are not required. That is the tendon will fail. Tests show it is virtually impossible to over-reinforce FRP prestressed T and I beams. (Section 8)

5.7.3.1.2 Components with Unbonded Tendons

C5.7.3.1.2

Very little research had been conducted on unbonded tendons. Equations in section 5.7.3.1.2 may be used with FRP tendons if a correction of E_f/E_s is added to the second term of the equation 5.7.3.1.2-1.

5.7.3.2 Flexural Resistance

C5.7.3.2

Add FRP equations for flexural strength.

Equations for flanged and rectangular sections are derived in Volume 1, Section 8. Equations are dependent on whether the section is over or under reinforced. Guidance for beams with vertically distributed tendons is provided.

5.7.3.3 Maximum Reinforcement

C5.7.3.3

FRP prestressing tendons can result in either over or under reinforced beam. The brittle nature of FRP tendons leads to a conclusion that either condition may be acceptable. Therefore, limits on the maximum amount of prestress are not applicable for beams with FRP tendons.

5.7.3.4 Control of Cracking by Distribution of Reinforcement

C5.7.3.4

Research has shown that the Gergely-Lutz Z factor is applicable to FRP tendons is the crack width or Z factor is increased by the ratio of the modulus of the steel tendon to the FRP tendon, E_s/E_f (Section 12).

5.7.3.5.1 Moment Redistribution

Moment redistribution is not allowed with FRP tendons.

No comprehensive research has been conducted to evaluate the effects of moment redistribution in beams with bonded FRP reinforcement. Moment redistribution due to the use of conventional steel reinforcement in the bridge deck should be permissible.

5.7.3.6.2 Deflection and Camber

C5.7.3.6.2

The effective moment of inertia, using the modulus of elasticity of the FRP tendon, is suitable for computing deflections for beams with FRP tendons (Section 14).

5.7.4.4 Compression Members Factored Axial Resistance

C5.7.4.4

Only pile tests have been conducted with FRP prestressing. The tests indicate that axial load and bending are predicted providing adequate confinement reinforcement is present.

No test data exists for high axial load or biaxial bending conditions (Section 10).

5.8.1 Shear and Torsion Design Procedure

C5.8.1

Section 15 provides an overview of beams containing FRP tendons and FRP stirrups. No data on torsional behavior is available. In general, the lowest value for v_c should be used and the stirrup capacity must be reduced by ϕ_{bend} to account for the stress concentration at the FRP stirrup bends.

With these corrections, the AASHTO shear design model appears adequate for beams with FRP tendons.

5.9 PRESTRESSING AND PARTIAL PRESTRESSING

5.9.1.5 CRACK CONTROL

Where cracking is permitted under service loads, crack width, fatigue of reinforcement, and corrosion considerations shall be investigated in accordance with the provisions of Articles 5.5, 5.6 and 5.7.

Beams presented with FRP tendons should be designed to be uncracked under service loads.

5.9.3 Stress Limitations for Prestressing Tendons

The tendon stress, due to prestress or at service limit states, shall not exceed the values:

• as specified In Table 1, or

• as recommended by the manufacturer of the tendons or anchorages.

The tendon stress at the strength and extreme event limit states shall not exceed the tensile strength limit specified in Table 5.9.3-1.

See Section 7.0. Glass tendons are not recommended due to the alkali reactivity of high stressed glass in concrete environments. The useful long-term tensile capacity of glass is probably about 20-30% of ultimate due to creep rupture. Glass tendons may be considered for post tensioning applications where the tendon is fully isolated from the surrounding concrete. (Section 6)

Table 5.9.3-1 – Stress Limits for FRP Prestressing Tendons		
	Tendon Type	
	CFRP	Aramid
At Jacking: (f_{pj}) -Pretensioning -Post-tensioning	0.65 f_{pu} 0.65 f_{pu}	0.50 f_{pu} 0.50 f_{pu}
After transfer: (f_{pt}) -Pretensioning -Post-tensioning – At anchorages and couplers immediately after anchor set -Post-tensioning - General	.60 f_{pu} .60 f_{pu} .60 f_{pu}	0.45 f_{pu} 0.45 f_{pu} 0.45 f_{pu}
At service Limit State: (f_{pe}) After losses	0.55 f_{pu}	0.40 f_{pu}

5.9.5 Loss of Prestress

5.9.5.1 TOTAL LOSS OF PRESTRESS

AFPR   = loss due to relaxation of FRP (KSI)

•See section 5.9.5.4.4b for relaxation of FRP tendons

Table 5.9.5.2.2b – Friction for Post-Tensioning Tendons

Recommended revisions to Table 5.9.5.2.2b-1

Type of Tendons and Sheathing	Wobble Coefficient, K (1/mm)	Curvature Coefficient, μ (1/RAD)
FRP Tendons in ridged and semi-ridged plastic ducts	0.0002	0.20

5.9-5-2.3 Elastic Shortening

5.9.5.2.3a Pretensioned Members

5.9.5.3 Approximate Lump Sum Estimate Of Time-Dependent Losses

C5.9.5.3

Lump sum estimates for FRP tendons have not been developed.

5.9.5.4 REFINED ESTIMATES OF TIME-DEPENDENT LOSSES

5.9.5.4.2 Shrinkage

C5.9.5.4.2

Correct shrinkage losses in eq. 5.9.5.4.2-1 the modulus of elasticity of the tendon compared to steel.

$$\Delta f_{PSR} = \Delta f_{PSR} \text{ (steel) } [E_f/E_S]$$

5.9.5.4.3 Creep

C5.9.5.4.3

Correct creep losses in eq. 5.9.5.4.3-1 by the ratio of the modulus of elasticity of the tendon compare to steel.

$$\Delta f_{PcR} = \Delta f_{PcR} \text{ (steel) } [E_P/E_S]$$

5.9.5.4.4 Relaxation

5.9.5.4.4a General

The total relaxation at any time after transfer shall be taken as the sum of the losses specified in Articles 5.9.5.4.4b and 5.9.5.4.4c.

5.9.5.4.4b At Transfer

Loss due to relaxation should be based on approved test data. If test data are not available, the loss may be assumed to be 31 MPa (4.5 ksi) for CFRP and 70 MPa (6.0 ksi) for AFRP.

C5.9.5.4.4b

The relaxation of FRP tendons comes from three sources, matrix relaxation, fiber straignthing, and fiber relaxation. The first two actions create a 2-3% loss. CFRP has no fiber relaxation beyond this. AFRP has an additive relaxation of 1% per 10 years

5.10.2 Hooks and Bends

5.10.2.1 STANDARD HOOKS

C5.10.2.1

FRP tendons are not to be bent

5.10.3.3.1 Pretensioning Strand

Pretensioning strands may be bundled, provided that the spacing, specified herein, is maintained between Individual strands. This provision shall apply to shielded and unshielded strand.

Groups of eight strands of 12 mm (0.5 –in) diameter or smaller may be bundled linearly to touch one another In a vertical plane. The number of strands bundled in any other manner shall not exceed four.

C5.10.3.3.1

Strands are often bundled at the harping point. FRP tendons may be harped providing the extra stress of bending at the harp is included in the stress calculations.

$$\Delta f = E_f \, (d_f/R)$$

where E_f = modulus of FRP tendon d_f is the tendon diameter and R is the radius of the harping saddle. A value of R > 0.9 m (30 in) is recommended.

5.10.9.1 GENERAL

C5.10.9.1

With slight modifications, the provisions of Article 5.10.9 are also applicable to the design of reinforcement under high load capacity bearings and for FRP tendon systems.

5.11.4.1 Bonded Strand

$$L_d \geq \frac{f_{se} d_b}{3} + \frac{3\left(f_{fu} - f_{se}\right)}{4} d_b$$

C5.11.4.1

Using f_{fu}, the equation predicts a longer L_d than current AASHTO in case of Technora. With Leadline and Strawman, it predicts a shorter L_d. (Section 16).

f_{fu}, the tendon rupture strength, should be used in place of f_{ps} in the equation. Doing so gives conservative predictions of L_d with all three composite tendons. Using f_{ps} will give less conservative results and possibly unconservative results as well.

5.11.5.2.2 Mechanical Connections	C5.11.5.2.2 There are no general use mechanical connections for FRP tendons.
5.12.3 Durability Concrete Cover	C5.12.3 FRP tendons do not corrode with the same mechanisms as steel. Therefore, cover requirements may be relaxed to more effectively use these materials. While FRP is recommended for highly corrosive environments, reduction of cover is not recommended unless a full durability is assured.
5.13.4.4.3 Precast Concrete Piles – Reinforcement	C5.13.4.4.3 Section 10 examines the fabrication, driving and testing of pile prestressed with FRP tendons and using FRP spirals. The test follows the AASHTO guidelines for spacing and number of turns of spiral ties. The tie diameter is approximately 0.2 in. The success of the test suggests that having FRP spirals equivalent to axial stiffness as the steel spiral provides satisfactory results.